Damage evaluation of H-section steel columns under impulsive blast loads via gene expression programming

Mohammad Momeni[a], Mohammad Ali Hadianfard[a,*], Chiara Bedon[b], Abdolhossein Baghlani[a]

[a] Shiraz University of Technology, Department of Civil and Environmental Engineering, Iran
[b] University of Trieste, Department of Engineering and Architecture, Italy

ARTICLE INFO

Keywords:
H-section steel columns
Blast load
Residual load carrying capacity
Support rotation
Finite Element (FE) numerical modelling
Gene Expression Programming (GEP)

ABSTRACT

Increasing terrorist attacks towards ordinary or strategic buildings and soft targets represent one of the major impetus to improve existing methods of design for blast-resistant structures. When a building undergoes an extreme dynamic event such as blast or impact, local damage of its key structural components (i.e., the columns) may lead to severe failure and even collapse of the entire building. Consequently, the availability of simplified, time efficient and reliable methods of analysis can be relevant for design. In this paper, H-section steel columns subjected to blast loads are numerically investigated, so as to derive practical formulations for damage evaluation assessment. The strategy is based on parametric Finite Element (FE) models (with up to 5600 configurations), validated towards experiments and, used as an extensive data bank, for further elaboration via Gene Expression Programming. Analytical formulations are in fact proposed for calculating some relevant parameters of design, such as (a) the initial and (b) the residual axial capacity of the examined columns. The collected results show that the proposed formulations can offer a good level of accuracy and high calculation efficiency for blast loaded H-section steel columns. In addition, an expression is proposed to relate the damage index (based residual axial capacity) to the conventional displacement/rotational index. Sensitivity analyses and some calculation examples are finally presented, to further investigate the potential of the approach for design purposes.

1. Introduction

In recent decades, due to the increase of terrorist attacks in human society, the continuous definition and refinement of accurate design methods for structures and load-bearing members under extreme dynamic loads (like blast and impact) has attracted a huge number of efforts. In buildings, columns are basic elements and play a crucial role in bearing design loads. In the case of extreme explosion events, the outer columns are even more vulnerable to damage compared to inner ones. Accordingly, the practical but time efficient and reliable evaluation of the possible damage scenarios due to impulsive loads represents one of the key aspects of design. Certainly, investigating the damage evolution in these members leads to a better understanding of their actual behavior in full 3D systems, and this turns out in an enhanced prevention of possible progressive collapse in buildings, and hence, allowing search and rescue operations after explosion.

Up to now, several field experiments and numerical studies have been performed by various researchers and institutions towards the fulfillment of optimal design approaches for columns exposed to combined gravity and wind loads, as well as accidental impacts like blast. Nassr et al. [1,2] carried out extensive field tests on a relevant number of wide flange steel columns excited by different blast loads, giving evidence of experimental results and numerical simulations. Magallanes et al. [3] investigated the behavior of a W360 × 347 steel column with a clear height of 5.73 m and subjected to 1818 kg of TNT equivalent ANFO, with a ground stand-off distance of 4.75 m. Later on, Nassr et al. [4] experimentally studied the dynamic response of eighteen Reinforced Concrete (RC) beams subjected to blast loading. In the mentioned literature documents (and others), one of the shared points of discussion and research has certainly been represented by the high cost of performing laboratory (or arena) blast tests on full-scale columns (or other load-bearing elements) under impact. This is why, from decades, the number of numerical studies based on equivalent Single Degree Of Freedom (SDOF) and / or even more detailed Finite Element (FE) methods has been continuously increasing, in order to calculate and evaluate the dynamic response and potential damage of several structural elements under blast loads [2,5–13]. In the other words, one of the feasible ways to quantify the effect of variability in input

* Corresponding author.
E-mail addresses: m.momeni@sutech.ac.ir (M. Momeni), hadianfard@sutech.ac.ir (M.A. Hadianfard), chiara.bedon@dia.units.it (C. Bedon), Baghlani@sutech.ac.ir (A. Baghlani).

Accepted 30 May 2020

parameters on the dynamic response of a structural system instead of performing high number of experiments is to model the structural system numerically, simulate the possible scenarios and developing some predicative equations.

There are two well-known criteria that can be used for the evaluation of damage in columns under blast, namely represented by (i) the support rotation and the (ii) damage index criterion based on the residual axial capacity. The support rotation approach represents the current basis of several standards and guideline books for the design of blast loaded structures (see for example [14,15]). As an alternative, the damage index criterion (based on the residual axial capacity) was proposed by Shi et al. [10] to estimate the post-blast damage of a given column, on the basis of its axial load bearing capacities before and after the incoming explosion. It is clear that since columns are primarily designed to carry axial loads, their residual capacity (i.e., criterion (ii)) should be able to better assess and represent the expected damage level. In this regard, several research studies have been carried out, aiming at assessing and estimating the effect of blast loads on the residual axial capacity of several structural components, including RC and strengthen RC columns [16–24], RC and ultra-high performance concrete-filled double-skin tubes columns [25–28], and steel columns [9,11,12,29–33]. A series of investigations have been dedicated to develop some empirical formulations to link some of the key parameters of design, such as the residual axial capacity and the calculated damage index for a given column. Bao and Li [16] carried out an extensive parametric numerical study to calculate the residual strength of blast loaded RC columns, by utilizing the LS-DYNA software. They proposed an empirical formula for predicting the expected residual capacity ratio of RC columns under blast, based on mid-height displacement to height ratios. Cui et al. [34] also assessed the damage evaluation in RC columns under close-in explosions, and proposed a relationship between the damage index (based on axial load carrying capacity) and the ratio given by the relative residual deflection over the column depth. Abedini et al. [18] defined an analytical expression, based on FE numerical analyses, to estimate the residual axial capacity of RC columns under blast. Wu et al. conducted an extensive parametric study to find some relationships between key input parameters (i.e., material mechanical properties and blast wave parameters) and the corresponding residual axial capacity of RC columns [21] and composite columns [35]. Some research studies [29–31] have been carried out and further extended, to find the failure probability of a given H-section steel column under different blast scenarios. Special care was given to the typical uncertainties associated with loading and material properties via an improved methodology based on Monte Carlo simulations in conjunction with LS-DYNA software analyses. Momeni et al. [33] recently investigated the typical behavior and dynamic performance of blast loaded steel columns with different cross sections via explicit FE analyses based on the LS-DYNA software. The authors showed that the comparative parametric FE results from (i) support rotation and (ii) damage index criteria tend to generally overestimate the expected damage level that would be expected from the displacement criterion; hence suggesting the latter as a more efficient design assumption. Furthermore, in the same project it was shown that the section shape for a blast loaded steel column has mostly null effects on the corresponding qualitative response, as far as the members are pinned at the ends. A maximum scatter up to 30–35% was also calculated for the same cross-section and load scenarios, as far as the support condition was changed from pinned to fixed ends.

The application of Artificial Intelligence (AI) methods like Artificial Neural Networks (ANNs), Gene Programming (GP) and an extension to GP as Gene Expression Programming (GEP) have received considerable attention in the field of civil engineering in order to solve complex problems where conventional computational techniques are incapable of giving a solution. In this regard, there are many dedicated research studies in which AI methods have been widely used and successfully established to find reliable solutions in the field of geotechnical [e.g. 36–41] and structural [e.g. 42–44] engineering as well as other branches of civil engineering. In the field of protective structures, a methodology based on ANNs – in conjunction with extended FE models – was proposed in [45] for W-section steel columns subjected to blast loading to develop a model which was able to capture their post-blast residual capacity. Remennikova and Rose [46] proposed and evaluated a new approach for predicting the blast environment behind a vertical blast wall by implementing the ANNs on a database of overpressures and impulses recorded during a series of small-scale blast wall experiments. Bewick et al. [47] utilized numerical simulation data generated from validated hydrocode simulations to train ANNs in order to predict the blast parameters on buildings protected by simple barriers. Hosseini et al. [48] carried out a comparison between the methods of (a) GP, (b) response surface method and (c) multivariate adaptive regression splines to build a reliable prediction for the peak particle velocity due to blast induced ground vibrations in quarry sites. Shin et al. [49] developed a framework by implementing ANNs to evaluate multi-hazard performance of non-ductile RC building frames and to mitigate their structural vulnerabilities using a retrofit system under combining seismic and blast loads. In [50], a formula was proposed to predict the maximum deflection of reinforced concrete panels subjected to the blast loads by implementing GEP and regression methods.

The application of FE methods for the prediction of blast loaded structural behavior has become essential in the evaluation of threats. Although the FE methods are robust and accurate, mostly these methods are time consuming and require a background in structural and blast engineering. On the other hand, in many cases, it is often necessary to evaluate structural response and their potential risks in a relatively short period of time, much faster than when a complex and nonlinear analysis is required. In this regard, simplified engineering tools, such as SDOF models, has been developed which is the basis of current books and codes of blast resistant design of structures. In strong explosions, because of localized behaviors and failures such as web buckling, flange deformations, and rupture of the web, SDOF methodology is not capable to describe or predict the response correctly. In this case, the use of FE methods becomes important and can be used in conjunction with computations algorithms like GEP to develop a fast-running model for predicting the structural response. Such a model can be used in reliability analysis of blast loaded structures (e.g. blast loaded steel columns) which demands high numbers of iterations [29,31,33].

In this paper, some equations are proposed to quickly predict the initial axial capacity and the residual axial capacity of blast loaded H-section steel columns, by implementing the GEP. In addition, a practical relationship is proposed to relate the damage index (based residual axial capacity) to the prevailing displacement/rotational ductility index. Such an outcome is achieved with the support of extended FE simulations carried out with the support of the LS-DYNA software. More in detail, a total of 5600 H-section steel columns is taken into account (in order to prepare data bank for GEP), where major variations are represented by the cross-section properties (in the range of IPB180 to IPB550), the loading scenarios (i.e., combination of blast and axial loads), variable material properties for steel, and different boundary conditions (pinned and fixed ends). A set of LS-PrePost, MATLAB, LS-DYNA and C# coding is also used in support of the parametric investigation, in order to link together a relevant number of input / output data of interest for automatic FE modelling, analysis of the models and extraction / post-processing of FE results. Finally, by creating an exhaustive database from all the collected FE results, the GEP method is implemented and a series of equations are presented, for both initial and residual axial capacities of blast loaded H-shaped steel columns. Finally, a sensitivity analysis is carried out to evaluate the model response towards possible variations in its input parameters. Some illustrative calculation examples are also presented, in order to show the practical applicability of the proposed equations for the design of steel columns under blast loads and for a reliable estimation of

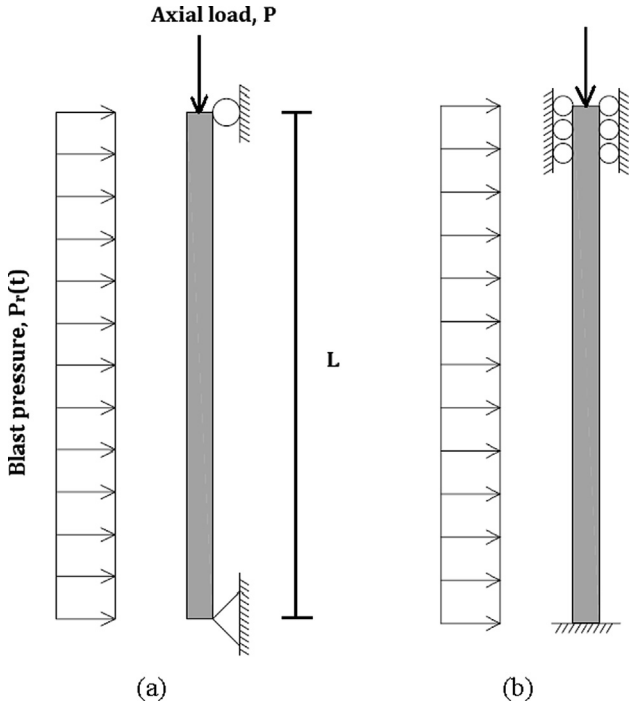

Fig. 1. Steel columns subjected to axial load and blast pressure, with (a) pinned or (b) fixed ends ().
reproduced from [33]

their expected damage level.

2. Blast load formulations, FE modelling and verification

The current research extends the investigation reported in [33], where the explicit FE software LS-DYNA was used to examine the behavior of H-section steel columns under the effects of axial and blast loads. A special care is taken into account, compared to the earlier study, to generate and analyze a wide set of parametric FE simulations (i.e. 5600 FE models) in order to create a comperhensive FE data bank for the derivation and assessment of practical formulations that can efficiently support the design of blast loaded steel columns.

In this regard, Fig. 1(a) and (b) schematically show the examined axially loaded steel columns, with pinned and fixed ends respectively, subjected to the given blast pressure. The top end of each column is considered axially unrestrained, in order to apply the desired axial load. Moreover, the blast load distribution is kept uniform along the columns' height [31,33].

To define the pressure time history of a blast wave, the exponential function of Friedlander's equation is used, that is:

$$P(t) = P_0 + P_{so}\left(1 - \frac{t - t_a}{t^+}\right)\exp\left(-\alpha\frac{t - t_a}{t^+}\right) \quad (1)$$

where P_{so} is the peak overpressure monitored for $t = 0$, P_0 is the ambient atmospheric pressure ($\approx$ 101.3 kPa) and α is a shape parameter. t^+, t^- and t_a are the positive phase duration, the negative phase duration and the arrival time, respectively. In this paper, the formulations presented in [33] are considered in order to determine the parameters of the Eq. (1).

To define steel material in LS-DYNA software, the MAT_PLASTIC_KINEMATIC (MAT_003) is then taken into account which is capable to describe the material strain rate effects through Cooper-Simonds relationship as follow:

$$\mathrm{DIF} = 1 + \left(\frac{\dot{\varepsilon}}{\mathrm{C}}\right)^{\frac{1}{\mathrm{P}}} \quad (2)$$

where DIF is Dynamic Increase Factor and $\dot{\varepsilon}$ is the material strain rate. The C and P constant coefficients of Eq. (2) were set equal to 40.4 and 5, respectively, as proposed in [51,52] for mild steel.

One of the most important issues in FE modelling is choosing the type of element for column simulating. The selected element type should be in such a way that it gives the most accurate result with the least amount of time-consuming. In this study, for FE modelling of steel columns, the fully integrated quadrilateral shell elements with five integration points through the thickness of each element, have been considered. Following the sensitivity analysis that has been done previously by the authors [33], the shell elements with maximum edge dimensions of 40 mm are selected for modelling of all steel columns. It is worth mentioning that, in FE modelling, the column flanges share nodes with the column web (i.e. merging duplicate nodes together) at the intersection between them.

To define boundary conditions and apply initial axial loading, two rigid plates were considered on the top and bottom of the column. For fixed ends, in the bottom of column, the rotations and translations of all nodes of rigid plate were constrained ($\delta_x = \delta_y = \delta_z = 0$ and $\theta_x = \theta_y = \theta_z = 0$). Moreover, for the top end, in addition to the conditions applied to the bottom rigid plate, the translation in the axial direction was also released ($\delta_x = \delta_y = 0$, $\delta_z \neq 0$ and $\theta_x = \theta_y = \theta_z = 0$) (see Fig. 2 (a)). Similarly, for pinned ends , on the bottom of column, all the nodes located on the horizontal centerline of rigid plate were

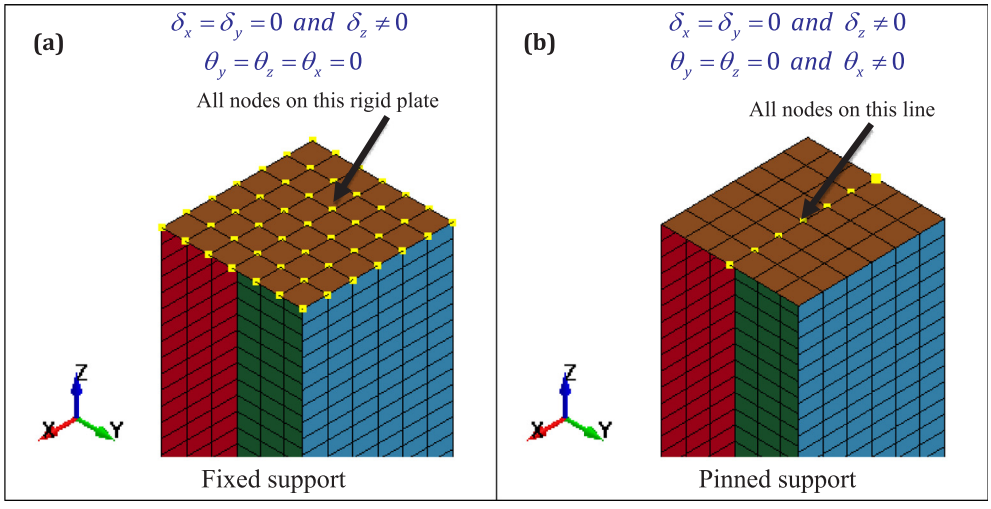

Fig. 2. Application of pinned and fixed support conditions in LS-DYNA.

constrained in all directions, with the exception of rotation around the x-axis ($\delta_x = \delta_y = \delta_z = 0$, $\theta_y = \theta_z = 0$ and $\theta_x \neq 0$); whereas for the top one, in addition to the conditions stated for the bottom rigid plate, the translation along the longitudinal axis was also released ($\delta_x = \delta_y = 0$, $\delta_z \neq 0$, $\theta_y = \theta_z = 0$ and $\theta_x \neq 0$) (see Fig. 2 (b)). The boundary conditions applied to each of the columns are individually selected as pinned and fixed ends. It is important to note that since the column support conditions in reality are neither fully pinned nor fixed, it is preferable for the designer to choose a value between the two perfectly pinned and fixed model values [31–33].

The accuracy and efficiency of the typical FE models were preliminary validated by taking into account the past experimental results of Nassr et al. (see [1,2]) and the numerical modelling strategy presented in [31,33] and the current study. For this purpose, two experimental tests were considered as “Test 1” and “Test 2”. The steel column specimens used in both experimental tests were manufactured from W24 × 15 with nominal length of 2.413 m under 270 kN of axial load. In “Test 1”, the column was subjected to 150 kg of ANFO at a stand-off distance of 9 m. In “Test 2”, the explosive charge and the stand-off distance were set to 50 kg and 10.3 m, respectively. The blast load parameters (i.e. blast pressure and positive phase duration) were defined conforming to the recorded values during the “Test 1” and “Test 2” by the sensors used in the experiments. In this regard, the average values of maximum reflective pressures were considered as 1560 and 307 kPa for Test 1 and Test 2, respectively. The average values for positive phase durations were also set to 6.2 and 7.3 msec for Test 1 and 2, respectively. These values were used to define the time history of blast loading in the FE models which was applied uniformly throughout the column height and for the full column width. Consequently, this results in a maximum peak of 159.12 and 31.31 N/mm for the time-varying load histories in “Test 1” and “Test 2”, respectively. According to the original test setup, the columns are modeled with pinned restraints (see Fig. 2(b)) and the bending deformations due to the imposed blast load shall occur about the strong axis. Regarding the mechanical properties of steel material, the steel used in the experimental specimens had a density of 7850 kg/m^3 and its yield strength, modulus of elasticity (MoE), Poisson's ratio and failure strain were equal to 470 MPa, 210 GPa, 0.3 and 0.2, respectively. The columns were simulated using shell elements with dimensions of 25 mm. The out-of-plane mid-span displacement time histories of experimental tests and those obtained from the FE models are shown in Fig. 3(a) and (b) for Test 1 and 2, respectively.

Based on Fig. 3, the maximum out-of-plane displacement in the mid-span of the columns obtained from the FE models are 30.15 mm and 4.98 mm for Test 1 and Test 2, respectively, which show a negligible scatter of –3.86% and −6.74% with respect to the 31.36 mm and 5.34 mm displacements of the experiments, respectively. Results obtained from validations show that the present FE model accurately predicts the column behavior under blast loads.

3. Post-blast residual axial capacity of column

Residual axial load carrying capacity of a column subjected to blast load, $P_{residual}$ represents the maximum amount of axial force that the column can endure after an explosion event. The four main stages should be followed as below to determine the $P_{residual}$ of a blast loaded column (see also Fig. 4).

(1) Gradually apply the primary axial load (as gravity load) to the column within a time period greater than or equal to 50 msec (time period of 75 msec is considered in this study) [10,53]. According to the past dedicated studies [10,31,53–55], the additional bending contributions caused by wind and gravity loads were ignored.
(2) Apply the lateral blast load to the column and perform dynamic analysis of the column.
(3) Continue the dynamic analysis after blast load until the column nodes meet the minimal velocities (zero value or less than 0.1 m/s in accordance with [10,31,53–55]) and damped vibrations.
(4) Gradually increse the axial load until the column fails [16]. The so estimated maximum axial force applied to the column at this stage is taken into account as the post-blast residual axial capacity of the column.

Fig. 4 schematically illustrates the stages mentioned above for finding $P_{residual}$.

According to Fig. 4, using the corresponding defined ramp function in stage 1, the primary axial load is gradually increased and applied to the top end rigid plate (see Fig. 2) with a uniform pressure so that the multiplication of this pressure by the rigid plate area is equal to ($\beta \times A \times F_y$) at time instant 75 msec, where A and F_y are cross

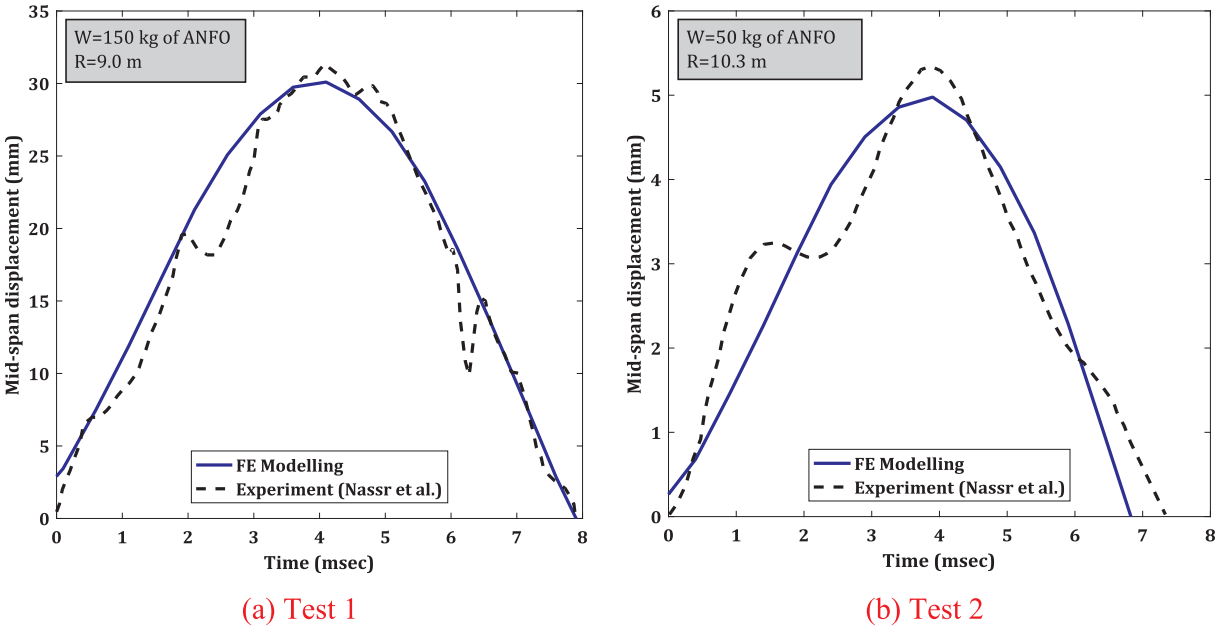

Fig. 3. Comparison the mid-span displacement time histories of the test columns obtained from the current FE analyses and the past experiments discussed in [2].

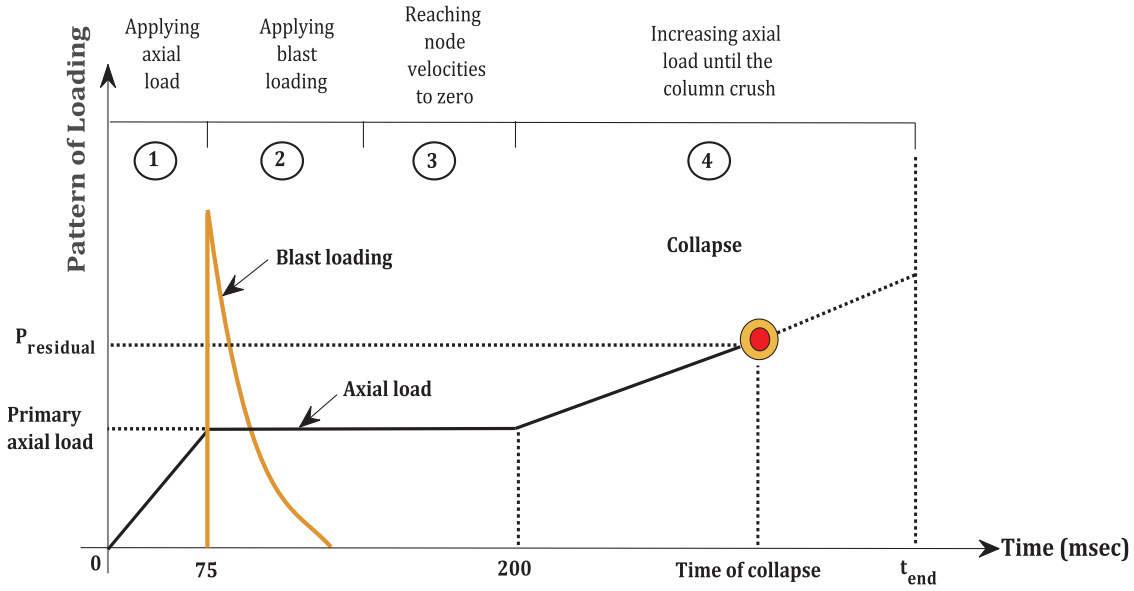

Fig. 4. Pattern of column loading stages in order to calculate the post-blast residual axial capacity [31] .

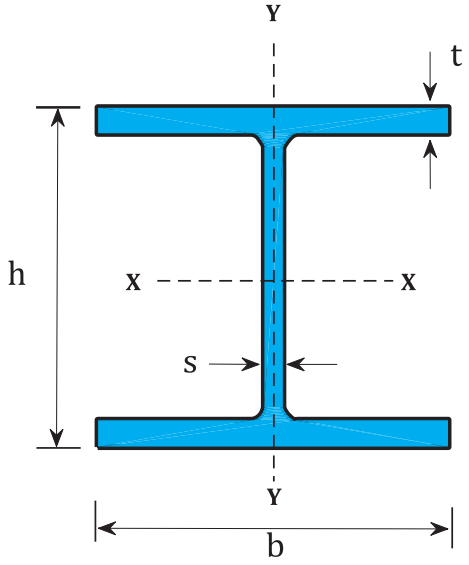

Fig. 5. Reference cross section for the selected H-section steel columns.

sectional area of the selected column and yield stress of steel material, respectively. The area of the installed rigid plate for each selected steel column is b × h, where b and h are the width and height of H-shape steel cross section, respectively (see Fig. 5). The parameter β is also defined as the ratio of primary axial load to the column's axial capacity and it falls within the range of [0.1–0.4] in this study (see Table 2). The loading rate in stage 1 depends on the geometrical and mechanical properties of the selected H-shape steel section and it is defined generally as ($\beta \times A \times F_y/75$) in the unit of kN/msec. As an example, the loading rate for the IPB300 steel column with $A = 14910\ mm^2$, $F_y = 240$ MPa, and $\beta = 0.2$ is approximately equal to 9.54 kN/msec. Subsequently, the loading rate in stage 4 is calculated as $(1-\beta) \times A \times F_y/(t_{end}\text{-}200)$ in the unit of kN/msec for each selected configuration. The parameter t_{end} represents the time instant at which the applied axial load approximately equals to the column's axial capacity and it is considered as 800 msec in this study. For the selected IPB300 steel column as an example, the loading rate is calculated as 4.77 kN/msec. The reduction in the loading rate of the fourth stage respect to the first stage is accomplished for the purpose of better capturing the post-blast nonlinear behavior of the column [31]. It is worth mentioning that the axial loading rates in stages 2 and 3 are zero. In the other words, the axial load remains constant in these stages and equals the primary axial load. Moreover, in the stages 1 and 4 no external dynamic load is applied and axial load of the column is gradually increased as quasi-static loading without impact effects.

4. Numerical simulation study

The behavior of different H-sections steel columns under blast loading is numerically investigated, based on a wide set of parametric FE simulations. For this purpose, a set of steel columns with different geometrical properties in cross sections (IPB180 to IPB550) and heights (2800, 3200, 3600, 4000 and 4400 mm) is considered in LS-DYNA. The overall geometric characteristics of the selected H-sections are shown in Table 1. In the table, A is cross sectional area, I_x is the moment of inertia about x-axis (strong axis), I_y is the moment of inertia about y-axis (weak axis), while other geometric parameters are shown in Fig. 5.

Recent blast incidents showed that most of explosions of terrorist attacks are classified based on the amount of explosive charge weights, and the distance of detonation from the structure. In FEMA 426 [56] and FEMA 452 [57], explosion magnitudes are classified according to the amount of explosives portable by human and different types of vehicles such as automobiles, vans and trucks [31]. In this regard, inspired by previous dedicated studies [17], the standoff distance and charge weight are assumed to be variable in the range of 4 to 20 m and 50 to 1000 kg, respectively. Since the explosion in terrorist attacks is assumed to occur on or near the ground surface, an instantaneous interaction between the blast waves and the surface ground forms the hemispherical surface burst. In this study, based on suggestions from [31,58–62], a conversion factor of 1.8 was used to find the effective charge weight (in kg of TNT) for estimating surface burst parameters using the free air burst formulas (with $W_{eff} = 1.8 \times W$). In other words, the effective charge weight for the FE simulations discussed in this paper varies between 90 and 1800 kg of TNT. Likewise, the axial load on the examined columns (which is applied as gravity load on the top of each member) is considered in the range of $[0.1–0.4] \times (A_g F_y)$. Finally, the yield stress is considered in the range of 210 to 470 MPa. The MoE of steel is kept fix to 210 GPa for all the FE configurations, based on the sensitivity analysis reported in [31] which also showed that MoE had negligible effect on the response of steel columns subjected to blast. Table 2 summarizes the input parameters used in the FE simulation of

Table 1
Geometrical properties of selected H-sections for parametric FE simulations.

	Section properties						
Identification	**b (mm)**	**h (mm)**	**s (mm)**	**t (mm)**	**A (cm^2)**	**I_x (cm^4)**	**I_y (cm^4)**
HEB 180	180	180	8,5	14	65,3	3831	1363
HEB 200	200	200	9	15	78,1	5696	2003
HEB 220	220	220	9,5	16	91,0	8091	2843
HEB 240	240	240	10	17	106,0	11,260	3923
HEB 260	260	260	10	17,5	118,4	14,920	5135
HEB 280	280	280	10,5	18	131,4	19,270	6595
HEB 300	300	300	11	19	149,1	25,170	8563
HEB 320	300	320	11,5	20,5	161,3	30,820	9239
HEB 340	300	340	12	21,5	170,9	36,660	9690
HEB 360	300	360	12,5	22,5	180,6	43,190	10,140
HEB 400	300	400	13,5	24	197,8	57,680	10,820
HEB 450	300	450	14	26	218,0	79,890	11,720
HEB 500	300	500	14,5	28	238,6	107,200	12,620
HEB 550	300	550	15	29	254,1	136,700	13,080

Table 2
Range of input parameters for the selected H-section steel columns.

Parameter	Range
Charge weight, W (kg of TNT)	50–1000
Stand-off distance, R (m)	4–20
Yield stress, F_y (MPa)	210–470
Initial load (consider as gravitational loads)	[0.1–0.4] × (A_gF_y)
Column heights, H (m)	2.8, 3.2, 3.6, 4.0, 4.4
IPB sections	180, 200, 220, 240, 260, 280, 300, 320, 340, 360, 400, 450, 500, 550
Support conditions	Pin-Pin and Fix-Fix

steel columns.

In the modelling of steel columns, creating a data bank for GEP, considering different possible scenarios and deriving predictive equations, the input values of explosive charge mass, stand-off distance, yield stress and axial load are randomly generated using the uniform distribution function in the range of parameters presented in Table 2. The assumption of choosing uniform distribution implies that there is some knowledge regarding the upper and lower bounds of the parameter values (see Table 2), but there is no information how their values are distributed and varied inside these bounds [63]. Also, the use of a uniform distribution allows each input parameter to take different values with same chance within a specified range. The following equation is used to generate uniformly random input parameters:

$$X = X_{\min} + rand \times (X_{\max} - X_{\min}) \quad (3)$$

where X is the random input parameter, X_{min} and X_{max} are the values of upper and lower bounds respectively and rand is a random uniformly distributed number between 0 and 1, which is generated through the use of the software MATLAB.

For each of the H-sections with a specific height and boundary condition (pin/fix), 40 different FE models are first produced randomly. For example, for a column with IPB180 section, height of 2400 mm and pinned ends, 40 FE model of columns are created in LS-DYNA software. Given that total number of five column heights are considered (see Table 2), for each section with a certain boundary condition (e.g. pin ends), 200 FE model of columns are totally produced. Noting that there are fourteen H-sections in the range of IPB180 to IPB550 (see Table 2), the total number of pinned models results in 2800 different configurations. Considering the other type of boundary condition as well (i.e. fixed ends), generation of 5600 numerical models for simulations is necessary. Since manual generation and handling such a huge number of FE models and results in LS-DYNA would be extremely hard and time consuming, a set of LS-PrePost, MATLAB, LS-DYNA and C# coding is used in this study to join together the key input data for automatic FE modelling, importing the models into LS-DYNA, extracting and post-processing the results. The technical steps for this kind of approach are listed as follows:

1. Selecting a number of generation (n_g = 40, in this study);
2. Selecting a steel section (from Table 2), with specific height and boundary condition (pinned or fixed);
3. Creating LS-DYNA model input file, for the selected steel column, in LS-PrePost software;
4. Generation of random variables (such as W, R, F_y) and axial load amplitudes (in the ranges of Table 2), using a uniform distribution function;
5. Calculating blast load parameters by employing generated W and R values (from step 4 and with the support of appropriate relationships);
6. Update the LS-DYNA model input file using MATLAB and C# coding. In other words, this step requires that all input parameters to be updated by random variables (already generated in step 3 and calculated blast load in step 4).
7. Analysis of the updated LS-DYNA model and collection of all the desired outputs (in this study, the maximum mid-span displacement and residual axial load carrying capacity of each column). This step is done automatically by linking LS-DYNA and C#;
8. Repetition of steps 2 to 7, until the number of simulated LS-DYNA models reaches the selected number of generation n_g (step 1).

The aforementioned steps are schematically described in the flowchart presented in Fig. 6.

5. Application of GEP for modelling residual axial load capacity

5.1. GEP procedure and the corresponding parameters

GP is one of the newest evolutionary computation algorithms or AI techniques which was proposed by Koza [64] in order to create computer programs based on the Darwinian principle of survival of the fittest [64]. An extension to GP is called GEP which was first developed by Ferreira [65]. AI models perform best when they do not extrapolate beyond the range of the data used for calibration. Therefore, it can be generally said that the aim of AI models is nonlinear interpolation within the data used for calibration [39]. With a given data set, in order to develop the best and robust AI models, all patterns contained in the data need to be included in the calibration set [66]. As an example, if the data set used for calibration does not include extreme data points of the available data, the developed model cannot be expected to perform well because the validation data set contains extreme data points and it

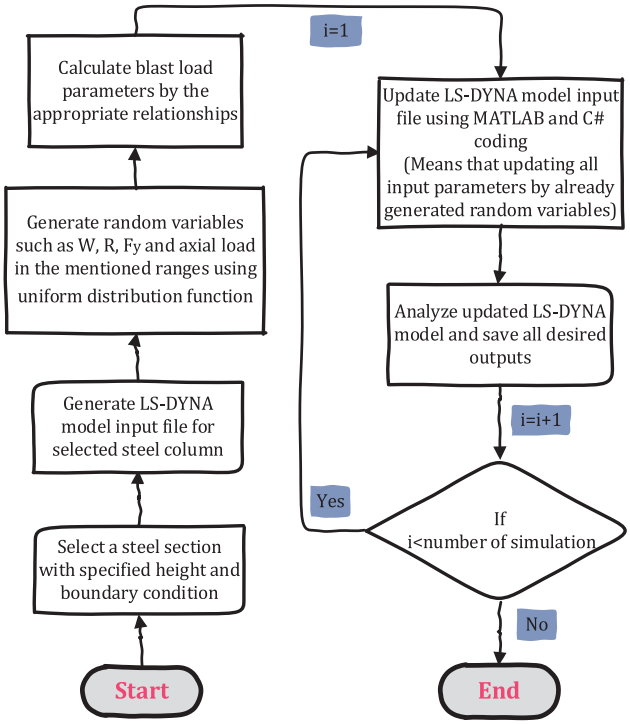

Fig. 6. Steps for the automatic generation of parametric models for blast loaded H-section steel columns.

will test the model's extrapolation ability rather than its interpolation ability [38–41]. Furthermore, the relations found by GEP can be used for both interpolating and extrapolating, but they have the best performance within the range of the data and there is no guarantee for the accuracy of the results beyond the mentioned ranges. In other words the accuracy of the results should be examined when GEP models are used for extrapolating. The GEP was implemented in this paper through GeneXpro Tools 5.0 [67] in order to find practical formulations for predicting initial and residual axial capacities of blast loaded H-section steel columns, based on input parameters and by performing a symbolic regression. To this aim, a large number of generations is needed to find a program that associates input parameters to outputs with the least amount of error and the highest level of accuracy. In this context, GEP is able to solve complex problems by encoding individuals of the created computer program in different programming languages (e.g. MATLAB, C++, FORTRAN, etc.), as linear strings of fixed lengths (the genome or chromosomes([68]. Each program consists of some Expression Trees (ETs) – where the number of ETs are defined by the user as genes numbers – with different sizes and shapes. Finally, the final formulation is extracted from these ETs. Generally, the performance of a GEP model depends on the required level of accuracy for the expected predictions. In [37], the effect of different linking functions was investigated based on the results of GEP model, showing that GEP performs best when the linking function is defined as "addition". Accordingly, the linking function is also chosen as "addition" in the current research study. Table 3 summarizes the key parameters and their corresponding setting which are taken into account for the GEP algorithm in GeneXpro Tools 5.0. It is worth mentioning that in order to find a formulation with the highest level of accuracy and the lowest level of complexity, special attention should be paid to select the number of genes, the number of chromosomes and the head size. Following the observations from previous dedicated studies in the literature, the numbers of chromosomes, genes, and head sizes were set equal to 30, 4 and 9, respectively.

Table 3
Optimal parameter settings for the GEP algorithm.

Parameter	Setting
Fitness function	RMSE
Number of Chromosomes	30
Number of Genes	4
Head size	9
Linking function	Addition (+)
Function set	+, ×, –, ÷, Inv, X^2
Mutation rate	0.044
Inversion	0.1
Transposition	0.1
Constants per gene	1.0

Table 4
Input and output statistics obtained using random data division for GEP1P.

Model variables and data sets	Statistical parameters				
	Mean	Std.	Min.	Max.	Range
Effective charge weight, W_{eff} (kg of TNT)					
Training	860.42	478.62	90.00	1800.00	1710.00
Testing	869.71	473.84	90.58	1799.13	1708.55
Validating	883.52	470.74	91.73	1794.94	1703.21
Stand-off distance, R (m)					
Training	12.50	4.49	4.00	20.00	16.00
Testing	12.45	4.52	4.07	19.95	15.88
Validating	12.63	4.57	4.16	19.96	15.80
Initial load, P_d (kN)					
Training	1424.62	767.35	149.50	4554.90	4405.40
Testing	1441.45	773.99	159.59	4537.43	4377.84
Validating	1444.25	783.91	165.54	4321.23	4155.69
Cross sectional area, A (mm2)					
Training	15969.92	5617.67	6530	25,400	18870.00
Testing	15779.82	5654.46	6530	25,400	18870.00
Validating	16256.45	5760.84	6530	25,400	18870.00
Yield stress, F_y (MPa)					
Training	339.54	74.95	210.00	470.00	260.00
Testing	342.36	74.48	211.91	469.52	257.61
Validating	340.80	77.49	210.80	469.86	259.06
Maximum slenderness, λ_{max}					
Training	52.93	11.16	36.93	96.31	59.38
Testing	52.10	11.23	36.93	96.31	59.38
Validating	52.00	11.36	36.93	96.31	59.38
Measured $P_{residual}$					
Training	5784.24	2591.28	327.93	12818.67	12490.74
Testing	5757.60	2534.54	138.40	12683.37	12544.97
Validating	5751.91	2544.85	851.86	12817.23	11965.37

5.2. A simple test problem by GEP

In order to validate the above-described approach, an illustrative example is presented to show capability of GEP in modelling complex real problems and finding accurate solutions. In this regard, the simple test function in Eq. (4) is chosen according to Ferreira [65]:

$$y = 3a^2 + 2a + 1 \tag{4}$$

Suppose a sample consists of the numerical values derived from Eq. (4) is given and the objective is to find the best function by using GEP procedure and compare with the known exact problem solution (i.e. Eq.4). This is actually a rather good and recognized aspect that allows to further appreciate the efficient results of blind operations in genetic operators [69]. However, this is obviously in contrast with real problems, where the target function unknown and represents the goal of calculation efforts.

In Eq. (4), the parameter a is the input independent parameter and y is the output dependent parameter. Over 10 randomly chosen points in the real interval [-10, +10] are provided in the form of ten pairs (a_i, y_i),

and the goal is to find a function which fits those values up to a certain accuracy. The sample data are set to those selected in [65], i.e. equal to −4.2605, −2.0437, −9.8317, −8.6491, +0.7328, −3.6101, +2.7429, −1.8999, 4.8852, +7.3998 for a_i values; and the corresponding y_i values can be easily calculated using Eq. (4). These 10 pairs are the fitness cases (the input) which will be used as the adaptation environment. The fitness of a particular program will depend on how well it performs in this environment [65]. There are five major stages in preparing to use GEP as follows.

In the first stage, the fitness function must be selected. For this problem, the following expression is chosen according to [65] to measure the fitness f_i of an individual program i and that is:

$$f_i = \sum_{j=1}^{n} (M - |P_{(i,j)} - T_j|) \tag{5}$$

where M is the selection range, P(i,j) is the value predicted by the individual program i for fitness case j (out of n fitness cases), and T_j is the target value for fitness case j. For this problem, if $|P_{(i,j)} - T_j|$ (the precision) is less or equal to 0.01, then the precision is equal to zero, and $f_i = f_{max} = n \times M$. The parameter M is set to 100 and therefore f_{max} equals to 1000 [65]. In the second stage, the set of terminals T and the set of functions F must be chosen to create the chromosomes. For this problem, the terminal set consists obviously of the independent variable, i.e., T = {a}. To determine the functions' set, there is no obvious way to select an appropriate function but a good guess can always be done in order to include all the necessary functions. In the present case, to make things a little easier, the four basic arithmetic operators are chosen, i.e. F = {+, -, *, /}. In the third stage, the chromosomal architecture including the length of the head and the number of genes must be chosen. In this problem these values are set to 7 and 3 per chromosomes, respectively. In the fourth stage, the linking function must be selected which is chosen as "addition" in this problem. In the final stage, the set of genetic operators and their rates must be chosen. In the present case, the genetic operators are set to mutation rate = 0.044, number of chromosomes = 30, constant per gene = 1.0, and for both gene inversion and transposition the rate of 0.1 is adopted.

To solve this problem, an evolutionary time of 50 generations and a small population of 20 individuals were chosen. All the individuals created in the evolutionary process can be completely analyzed and encoded, but for the sake of conciseness, only the best solution is presented. Fig. 7 shows the average fitness and the best fitness of individuals during evolutionary process. As can be seen in Fig. 7, a perfect solution is found in generation 4 with the best individual fitness 1000.

The ETs of the best individual of generation 4 is shown in Fig. 8. This figure reveals that the final extracted formula which can be obtained easily by linking the three sub-ETs with addition (i.e y = (Sub-ET1) + (Sub-ET2) + (Sub-ET2)) is exactly equal and match to the target test function given in Eq. (4). The results of this simple test problem show that GEP can be generalized and used for modelling complex real problems and finding reliable solutions.

5.3. Data bank for GEP modelling

The residual axial capacities of 5600 FE steel columns are employed to develop the prediction models for residual axial capacity of H-section steel columns subjected to blast loading by implementing GEP software (i.e., a set of 2800 FE models for pinned boundary conditions and 2800 FE models for fixed restraints). In doing so, up to ≈70% of each dataset is used as training data, 15% as testing data, and the remaining output as validating data set [68]. It should be noted that the division of database is performed randomly but the statistical consistency of the data subsets are also taken into consideration [40,65,70–73]. In doing so, the data set is divided so that to ensure the statistical properties (i.e. mean, standard deviation, minimum, maximum, and range) of each subset are close enough to each other. This ensures that the data used in

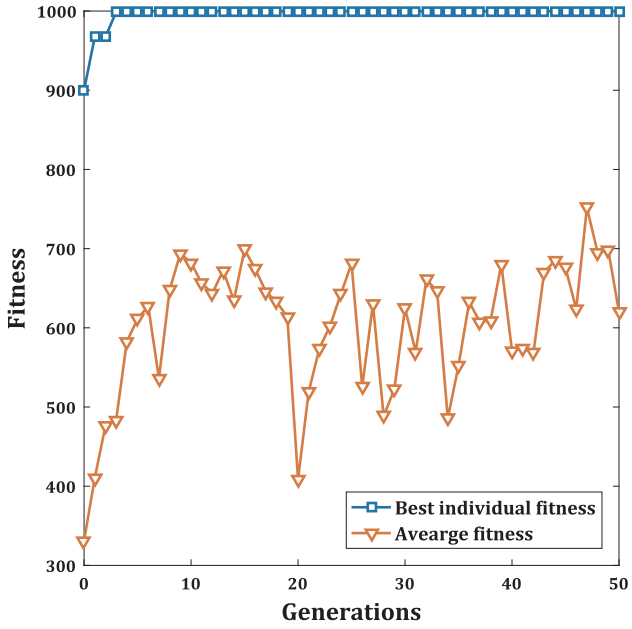

Fig. 7. Progression of average fitness of the population and the fitness of the best individual.

the different subsets are representative of each other which means the performance of the developed models are similar on each of the three subsets, indicating model interpolation ability rather than extrapolating within the available data [39,40]. A trial and error process is conducted through several GEP runs to reach this point and to find the models with the best performances. As an example, for one of the proposed formulas which will be presented later in Section 5.4 as the GEP1P model (see Tables 6 and 7), the statistics of the data used for training, testing and validating sets are presented in Table 4. According to the table, although the data are randomly divided, there is a statistical consistency between the data sub sets selected for each parameter in training, testing and validating stages. In the other words, the statistical properties of the selected sub sets are similar to each other with a confidence level of more than 95% which means that the maximum scatters between the Mean and Std. values of selected sub sets for each input parameter are less than 5% (e.g., for W_{eff} the maximum scatters between Mean and Std values of all training, testing and validating subsets are 2.61% and 1.65%, respectively) [40,74]. This is due to the fact that the database is comprehensive enough and all subsets are representative each other. Furthermore, in all cases, the training subsets include extreme values to ensure the best performance of the proposed models, since as mentioned earlier, the GEP models are more efficient for interpolation within the range of available data.

It should be also noted that each component of the data set is normalized using a max–min approach by Eq. (6), so as to lie in an interval of [0, 1] in order to change the values of dataset to a common scale without distorting differences in the ranges of the values which leads to better predictions:

$$X_{norm} = \frac{X - X_{\min}}{X_{\max} - X_{\min}} \tag{6}$$

where X_{norm} are the normalized values for the X-th parameter.

While there are various criteria for fitness function evaluation in GEP models, Root Mean Square Error (RMSE) is usually used. To assess the performance, accuracy and efficiency of the final formulations, R-squared values (R^2) are calculated for training, testing and validating data. The greater the R^2-value, the more precise the proposed model. RMSE and R^2 can be calculated as the following equations:

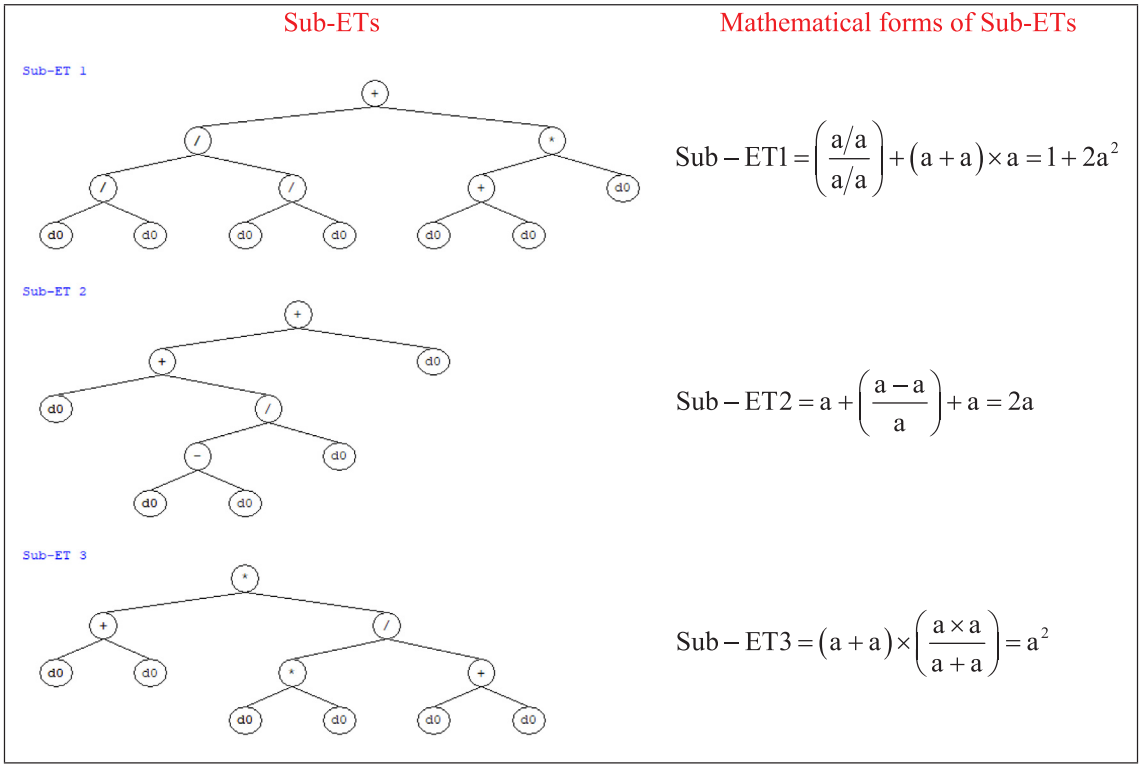

Fig. 8. Perfect solution to the simple target function using GEP.

Table 5
Parameters and characteristics of different GEP models and used variables in both Pinned and Fixed conditions.

Boundary Condition	Model Name	Number of genes	Used variables				
			W_{eff}	R	P_d	λ_{max}	$A.F_y$
Pinned	GEP1P	4	●	●	●	●	●
	GEP2P	4	●	●	●	●	●
	GEP3P	4	●	●		●	●
Fixed	GEP1F	4	●	●	●	●	●
	GEP2F	4	●	●		●	●
	GEP3F	4	●	●	●	●	●

$$RMSE=\sqrt{\frac{1}{n}\sum_i (t_i-o_i)^2} \tag{7}$$

$$R^2=1-\left(\frac{\sum_i (t_i-o_i)^2}{\sum_i (o_i)^2}\right) \tag{8}$$

where t_i is the target parameter (here, the residual axial capacity obtained by FE modelling), o_i is the output parameter (here, the residual axial capacity obtained by GEP models) and n is the number of dataset.

5.4. GEP results

One of the advantages of the GEP technique is that the relationship between the inputs parameters and the corresponding outputs is automatically constructed in the ETs. For example the ETs obtained for one of the model of residual axial capacity of blast loaded H-section steel columns with pinned ends condition is shown in Fig. 9. In this figure, d0, d1, d2, d3 and d4 are effective charge weight (W_{eff}), stand-off distance (R), maximum slenderness (λ_{max}), production of yield stress and cross sectional area ($A.F_y$), and initial axial load (P_d), respectively. The other parameters are constant values calculated by GEP which are different in each sub-ETs. By considering the fact that addition linking is used in this study, the final formulation of each of GEP models can be defined by adding all sub-ETs together (see Fig. 9).

In order to find a high performance model with the highest R^2-value, a huge number of trials was carried out (not presented in this paper, for the sake of conciseness) for blast loaded H-section steel columns, with both pinned and fixed boundaries, and only the best predictive models are presented herein. Table 5 shows the characteristics of all GEP models, their difference and their variables, for both pinned and fixed ends. By introducing all constant values in the Sub-ETs, the final equations of all six proposed GEP models for residual axial capacity are hence simplified, and presented in Tables 6 and 7 (for pinned and fixed ends, respectively). As can be seen from Tables 6 and

Table 6
Proposed equations for residual axial capacity in pinned end condition.

Model	Equation of $P_{residual}$	Training R^2	Testing R^2	ValidatingR^2	Number of involved variables
GEP1P	$P_{res}=\frac{0.094(7.66+R)(R-W_{eff})}{7.09-R}+AF_y+0.46R^3(R-\lambda_{max})(W_{eff}-AF_y)AF_y\cdots$ $+2(W_{eff}-0.32)\lambda_{max}{}^2AF_y{}^3-0.33W_{eff}\lambda_{max}{}^2AF_y(3.56+W_{eff}-2P_d)$	0.956	0.954	0.951	5
GEP2P	$P_{res}=0.04R(2+R)-0.13W_{eff}+AF_y+\frac{\lambda_{max}(2\lambda_{max}+RAF_y)(P_d-AF_y)}{AF_y+3.2}+\frac{R(W_{eff}-(\lambda_{max}+P_d)^2)}{(R-4.74)^2}$	0.952	0.951	0.942	5
GEP3P	$P_{res}=AF_y+W_{eff}\lambda_{max}{}^2(AF_y-1.44)AF_y+0.01(-5.97+AF_y)(W_{eff}-2R+AF_y)$	0.951	0.949	0.944	4

Table 7
proposed equations for residual axial capacity in fixed end condition.

GEP Model	Equation of $P_{residual}$	Training R^2	Testing R^2	ValidatingR^2	Number of involved variables
GEP1F	$P_{res} = -0.036(1.31 + W_{eff})(W_{eff} - R) + AF_y + \frac{RAF_y}{R - 5.78 + 4.82W_{eff}(AF_y - 2.34)}\cdots + \frac{0.102}{2.43 - R + 0.5\lambda_{max} - 0.5P_d} + {\lambda_{max}}^2 AF_y\left(0.2P_d - \frac{0.48W_{eff}}{W_{eff} + R}\right)$	0.981	0.984	0.984	5
GEP2F	$P_{res} = 0.053{W_{eff}}^2(R - 1.053)(R + 3.63)\lambda_{max} + 0.036R^2(1.8 + W_{eff} - 3.AF_y)\cdots + AF_y + \frac{1}{(22.03 + 8.28W_{eff})(2W_{eff} + \lambda_{max} + 2.50AF_y)}$	0.980	0.983	0.984	4
GEP3F	$P_{res} = 0.08R - 0.05W_{eff}(W_{eff} - R^2 - AF_y) + AF_y - \frac{R^2AF_y(\lambda_{max} + AF_y)}{P_d + 6.11} - \frac{W_{eff}\lambda_{max}(W_{eff} - R + AF_y)}{P_d + 10.74}$	0.978	0.982	0.983	5

7, all five input parameters were not used in all models. In some cases, four variables were selected to model the residual axial capacity with satisfactory accuracy compared to the models which employs all five parameters. It is worth mentioning that the proposed formulations are applicable for standard H-section steel columns with $0.5 \leq b/h \leq 1.0$, where b and h are previously shown on Fig. 5. However, for b/h ratios outside this range, more comprehensive studies are required.

Figs. 10 and 11 show the predictions of all GEP models in training, testing and validating parts for pinned and fixed ends conditions. As Figs. 10 and 11 indicate, all proposed GEP models are capable of predicting the residual axial capacity of a given H-section steel column with satisfactory accuracy close to FE results. However, it is obvious that besides the capability of satisfactory prediction of a desirable property by a given formula, the simplicity and ease of use of the proposed equation is also important. Tables 6 and 7 propose six different equations (three equations for each type of boundary condition) for this purpose with different level of complexity. The accuracy of each proposed model in predicting the residual capacity of a given H-section is also shown in the tables by reporting R^2 values for training, testing, and validating data. As the tables reveals, the R^2 values in all cases are more than 94%, indicating very satisfactory accuracy of predictions by the proposed formulas for the residual axial capacity of the selected columns (usually, R^2 values more than 80% are considered to be satisfactory). The maximum values of R^2 in the training, testing and validating stages are 0.956, 0.954 and 0.951, for pinned condition (GEP1P model), respectively, and 0.981, 0.984, 0.984 for fixed condition (GEP1F model), respectively.

In addition to the equations presented in Tables 6 and 7 for the reliable estimation of the residual axial capacity, the research study is further extended for presenting two additional equations to predict the initial axial capacity of the same H-section steel columns. For this purpose, the initial axial capacities of all the column models under blast loads are used again. In doing so, all the column models are further analyzed regardless of the explosive load; thus the FE values related to their initial axial capacity are extracted and used as a new data bank for developing the required formulations. The same strategy is considered similar to that adopted for developing residual capacities' equations for data division. In this regard, each database is first normalized using a max–min approach, then 70% of each dataset is randomly selected and used for training, 15% for testing, and 15% for validating. After using the aforementioned database in GEP, Eqs. (9) and (10) are proposed as follow to calculate the initial axial capacity of H-section steel columns in the case of pinned and fixed ends, respectively. Although various relations are found by GEP, formulas with the best performances are only presented here for the sake of brevity.

$$P_{initial\_Pinned} = A - A^2{\lambda_{max}}^2 + 0.177F_y + 0.388A(A\lambda_{max} + F_y - 1.575)\cdots +0.0176(A - \lambda_{max})(0.0535 - A + F_y + {F_y}^2) \quad R^2 = 0.997 \tag{9}$$

$$P_{initial\_Fixed} = A + \frac{F_y}{5.089 - 2.605A + F_y} + \frac{4A(F_y - 2.018)}{12.878 - \lambda_{max} + F_y} \quad R^2 = 0.998 \tag{10}$$

It is reminded that to determine the initial axial capacity of an H-section column by using Eqs. (9) and (10), and the residual axial capacity by using equations reported in Tables 6 and 7, the input values for the parameters should be first normalized. The range of input parameters used in FE models and adopted for GEP prediction formulas are presented in Table 8.

It should be noted that, the predicted values for residual axial capacity and initial axial capacity based on the proposed equations are normalized values and must be de-normalized to give the final prediction. In this regard, the following equation must be used:

$$X_{De-normalized} = X_{Normalized}(X_{max} - X_{min}) + X_{min} \tag{11}$$

where $X_{Normalized}$ is the normalized output based on the proposed equations, X_{max} and X_{min} are the maximum and the minimum measured values for parameter X obtained from FE results, respectively (i.e. residual axial capacity and initial axial capacity) and $X_{De\text{-}normalized}$ is the final predicted de-normalized value of parameter X. Table 9 shows the minimum and maximum values of initial and residual axial capacities of the simulated columns for both pinned and fixed ends conditions.

6. Sensitivity analysis

Sensitivity analysis refers to change inputs or model parameters, to evaluate the behavior of a model and to ascertain the dependence of its outputs on its input parameters [31,75,76]. Following Section 5, a sensitivity analysis is carried out to determine the model response with respect to the changes of input variables to find the most and the least effective parameters. For this purpose, the mean value of one of the input variables is increased (i.e., New mean = Old mean + 5% Old Mean) while the ranges of all other parameters are maintained constant (i.e. Mean value) and accordingly the amount of changes in the objective function (P_{res}) is then measured. In this regards, the GEP1P and GEP1F models are selected for pinned and fixed conditions, respectively and consequently the results are shown in Fig. 12(a) and (b). As can be seen, by increasing the R and AF_y parameters, p_{res} increases, while by increasing W_{eff} and λ_{max}, the value of P_{res} decreases. Furthermore, it is possible to see that P_d has negligible effect on the P_{res} values, compared to other input parameters; while AF_y is the most influencing parameter in the model.

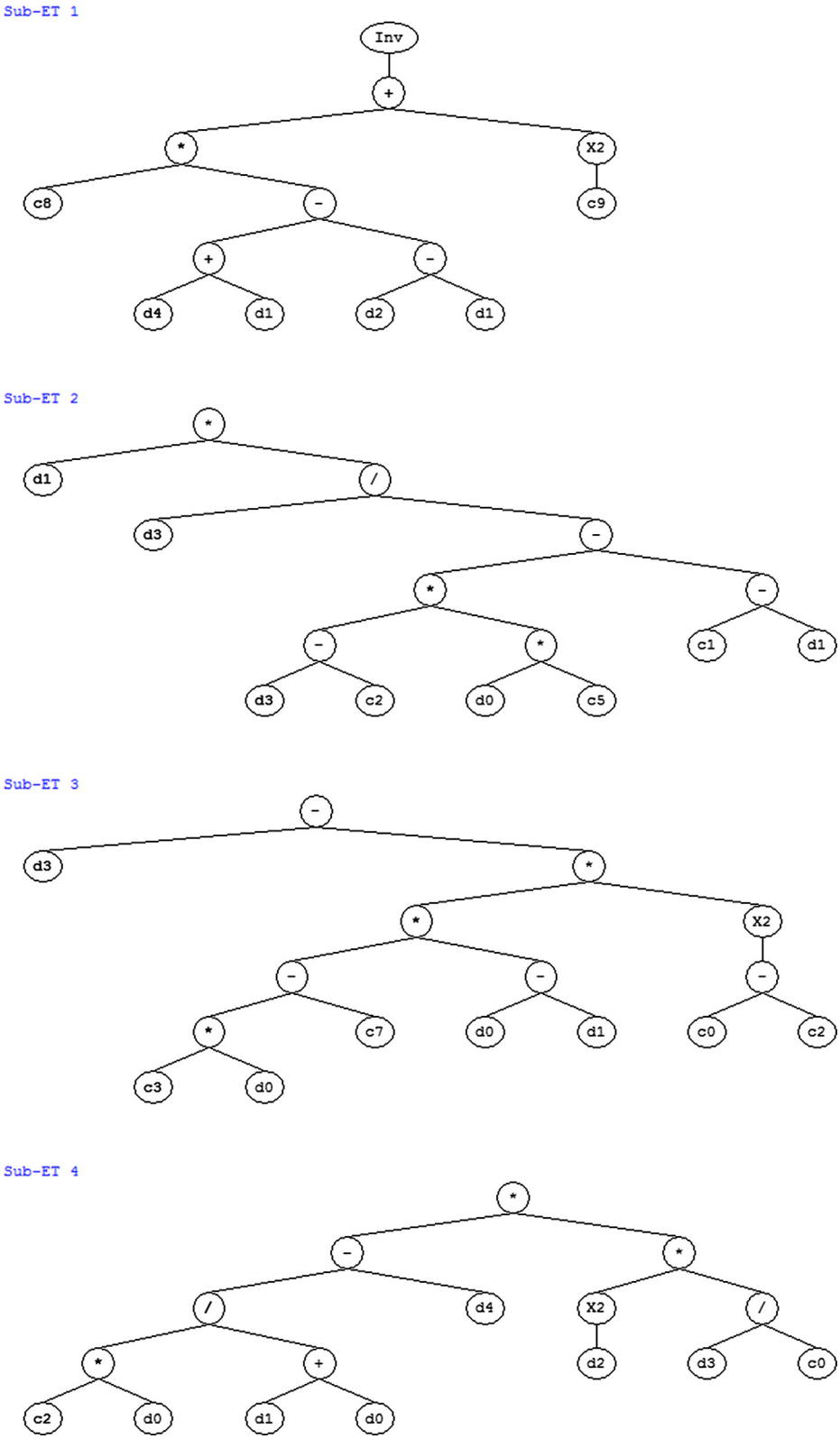

Fig. 9. ETs for one of the GEP models of residual axial capacity (Final ETs = (Sub-ET 1) + (Sub-ET 2) + (Sub-ET 3) + (Sub-ET 4)).

7. Relation between damage index and support rotation criteria

In the design of a structure (or a structural member) subjected to blast loads, the performance-based design approach is conventionally taken into account. In other words, the deformations determine whether the selected member has acceptable performance against the imposed blast pressure or not. The expected support rotationθrelates maximum deflection of a member to its length and is defined as the angle formed between a line connecting the member endpoints and a line joining the element where the deflection is maximum to the supports (see Fig. 13) [14,15]. In the other words, the expected support rotation typically results from a combination of the maximum

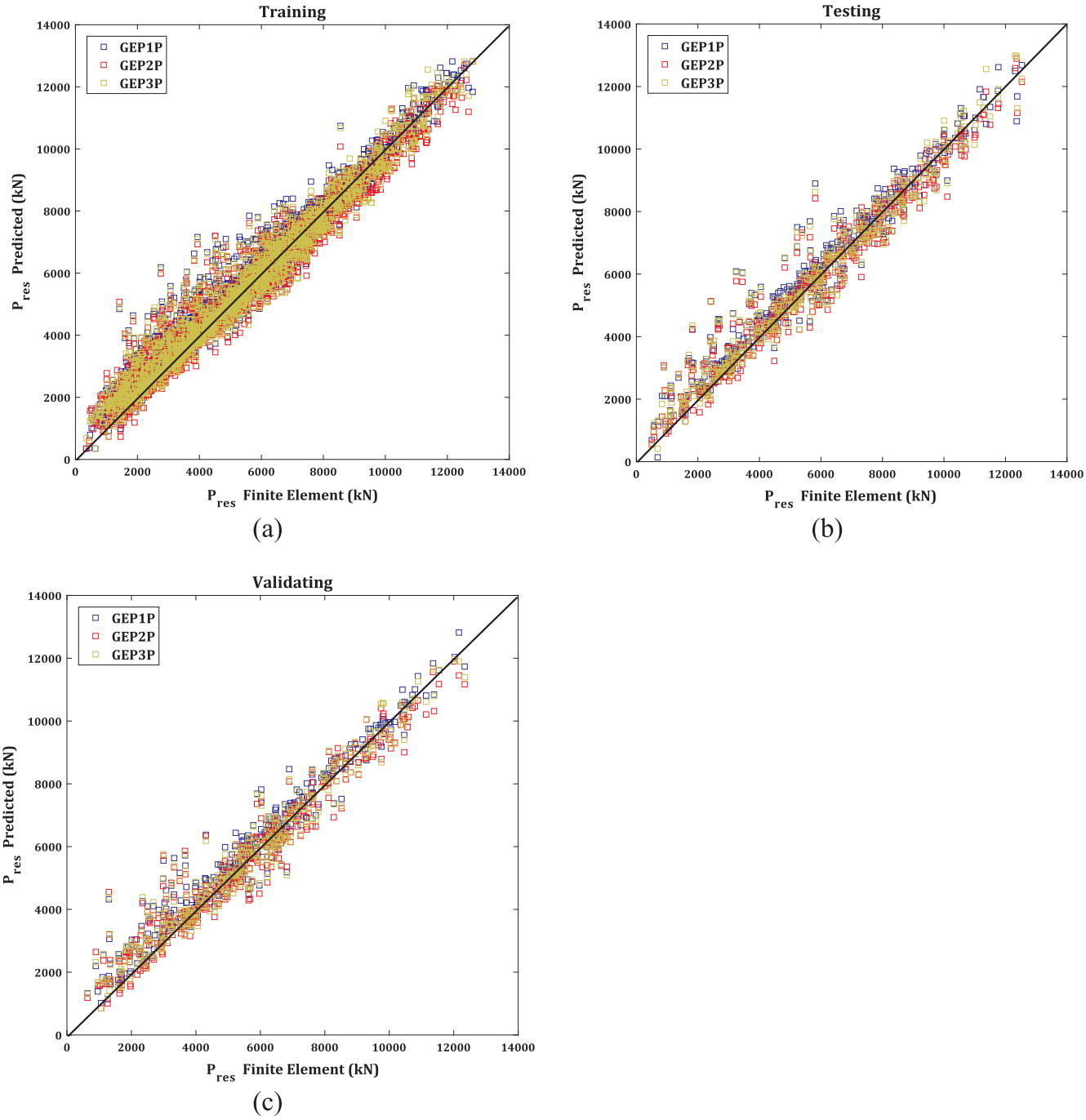

Fig. 10. Comparison of $P_{residual}$ values obtained from finite element analysis and proposed relationships for pinned boundary conditions, (a) Training, (b) Testing, (c) Validating.

displacement y_{max} of a given column, and of the column length L, that is [14]:

$$\theta = \tan^{-1}\left(\frac{y_{max}}{0.5L}\right) \tag{12}$$

The so estimated rotation amplitude shall be then compared with a set of limit values given by standards, like, for example, the UFC-3-340-02 provisions [14], where the support rotation criterion is recommended as a suitable design method for blast loaded steel members (see Table 10).

On the other hand, damage index based on the residual axial capacity of the damaged structure (structural member) represents one of the most important parameters for design and the most reliable estimate of damage, i.e. the remaining post-blast life of the structure or the maximum amount of axial force that the column can withstand after an explosive event, in order to resist against progressive collapse and provide structural stability during search and rescue operations. Damage index is a non-dimensional value between 0 and 1 (or 0% and 100%) and can be calculated experimentally or theoretically, based on computationally efficient FE methods using the following equation:

$$DI = 1 - \frac{P_{residual}}{P_{initial}} \quad or \quad DI = 100 \times \left(1 - \frac{P_{residual}}{P_{initial}}\right) \tag{13}$$

where $P_{residual}$ is the residual axial capacity of the damaged column after the explosion and $P_{initial}$ is the maximum axial load-carrying capacity of the undamaged column. The degrees of damage are classified into four

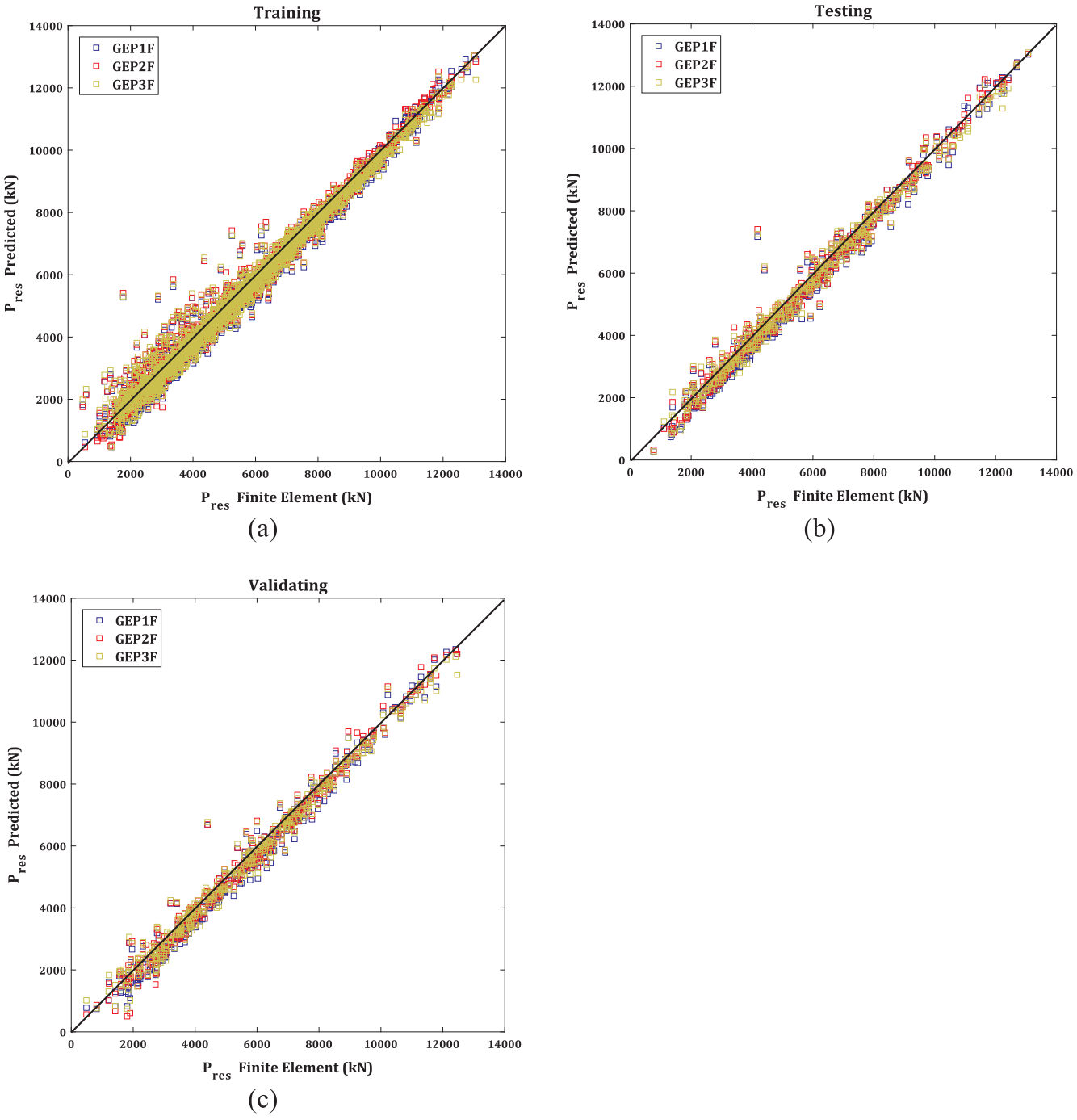

Fig. 11. Comparison of $P_{residual}$ values obtained from finite element analysis and proposed relationships for fixed boundary conditions, (a) Training, (b) Testing, (c) Validating.

Table 8
The range of input parameters.

Property	Range	
W_{eff}	90–1800 (kg of TNT)	
R	4–20 (m)	
A	6530–25400 (mm^2)	
F_y	210–470 (MPa)	
λ_{max}	For Pinned	36.93–96.31
	For Fixed	18.47–48.15
P_d	149.5–4554.9 (kN)	

Table 9
Minimum and maximum values of $P_{residual}$ and $P_{initial}$.

Property	Boundary condition	Minimum value (kN)	Maximum value (kN)
$P_{residual}$	Pinned	101	12,819
	Fixed	469	13,048
$P_{initial}$	Pinned	1538	13,016
	Fixed	1551	13,061

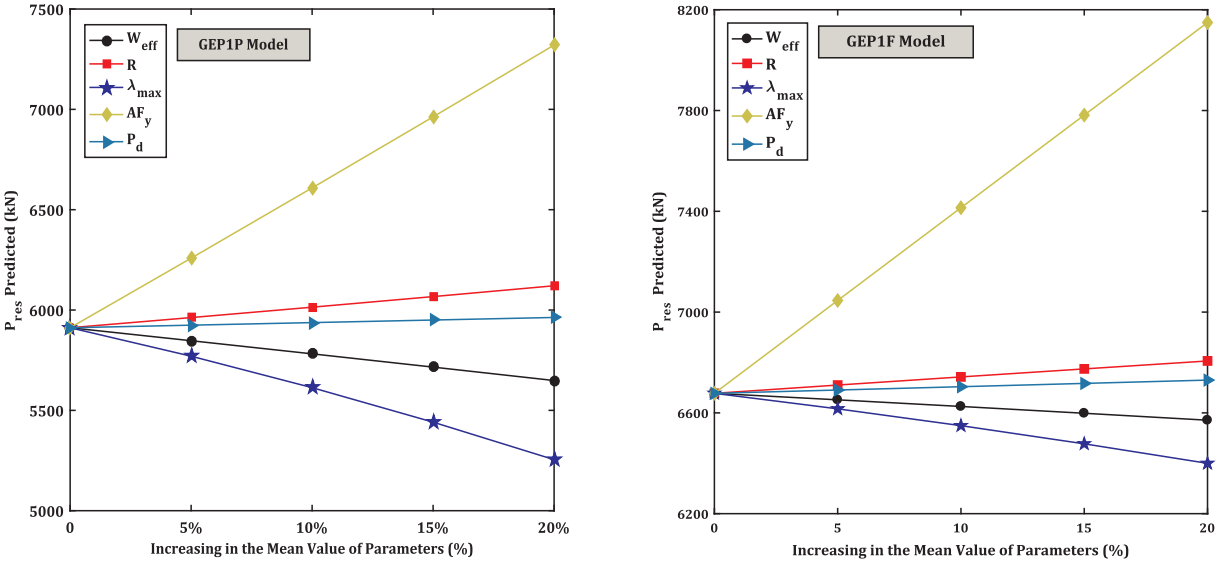

Fig. 12. Results of sensitivity analyses; (a) Pinned (b) Fixed ends condition.

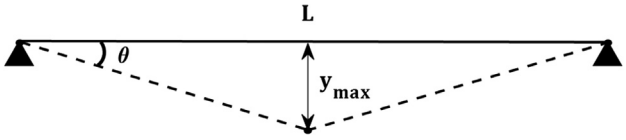

Fig. 13. Component of support rotation.

Table 10
Expected damage level for primary steel frame members, according to UFC provisions [15], based on support rotation.

	Component	Level of damage		
		Low	Medium	High
Maximum allowable support rotation (in degrees)	Steel primary frame members (without significant compression)*	1^0	2^0	4^0
	Steel primary frame members (with significant compression)*	1^0	1.5^0	2^0

* = "Significant compression" is associated to an axial compressive load that exceeds up to 20% of the dynamic axial capacity of the member.

levels [10]:

a) DI = 0–0.2 (or 0–20%) low damage
b) DI = 0.2–0.5 (or 20–50%) medium damage
c) DI = 0.5–0.8 (or 50–80%) high damage
d) DI = 0.8–1.0 (or 80–100%) collapse

when DI value falls between one of the mentioned ranges, regardless of its magnitude, it reports only one specific case of damage corresponding to that level.

$P_{residual}$ is derived from a FE analysis, whereas there are two ways to calculate $P_{initial}$. The first method is based on equations presented in regulations [77] and the second can be obtained through numerical analysis with appropriate software like LS-DYNA. In this study, both $P_{initial}$ and $P_{residual}$ are calculated using the latter method. To calculate $P_{initial}$, the axial load, when no blast is assumed to exist, is applied gradually until the column reaches its maximum axial bearing capacity.

To calculate the support rotation of a structural member under impulsive blast load, the conventional SDOF (this method is not capable to evaluate post-blast behavior) or FE method (i.e., without capturing the post-blast behavior of column) can be used, which require less computational effort compared to evaluating damage index (based on residual axial capacity which needs capturing post-blast behavior of column) by FE method. On the other hand, as stated earlier, since columns are primarily designed to carry axial loads, their residual axial capacities and consequently their damage indices assess the expected damage level and post-blast behavior of columns more precisely compared to support rotation criterion. In this regard, the goal of the latter research stage was to find a relationship between support rotation and damage index criterion estimates. According to the above explanations, such a relationship can simultaneously fulfill two conditions, namely:

(i) Reducing time of analysis (by calculating support rotation value as an input parameter which requires less computational effort compared to damage index criterion);
(ii) Increasing accuracy in predicting the damage by modifying the damage predicted by support rotation criterion and relating it to the damage index criterion (better estimation of damage by calculating damage index value as an output parameter).

For this purpose, the values of support rotation and damage index of 5600 steel columns under blast are extracted for both pinned and fixed members, and used as an exhaustive data bank for further elaborations. Fig. 14 represents the values of damage index versus support rotation (in degrees), as extracted from FE results, and calculated by Eqs. (12) and (13), respectively. To provide such a relationship, it must first be determined that for what value of the support rotation, can be said with certainty, both damage criteria predict the same level of damage for blast loaded steel columns. According to Fig. 14, the support rotation value corresponding to DI = 0.8 (i.e. the boundary value between high damage and collapse) is calculated as 8 degrees. This means that for support rotations greater than 8 degrees (see Table 10), both damage criteria predict the collapse level. On the other hand, for support rotations values less than or equal to 8 degrees, the predicted damage based on support rotation criterion should be modified by the proposed relation to obtain more realistic damage estimations (see also Figs. 15 and 16 for visual information). In Fig. 14, a relationship for damage index based on support rotation is also derived with the support of Matlab curve fitting, by using a Fourier function of existing data (withR^2 = 0.957 and RMSE = 0.0329). Its final expression takes the form of Eq. (14).

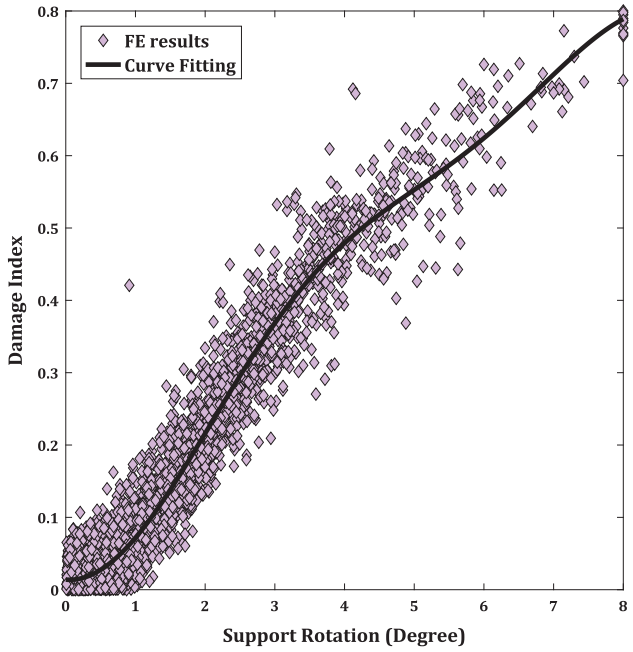

Fig. 14. Damage index versus support rotation.

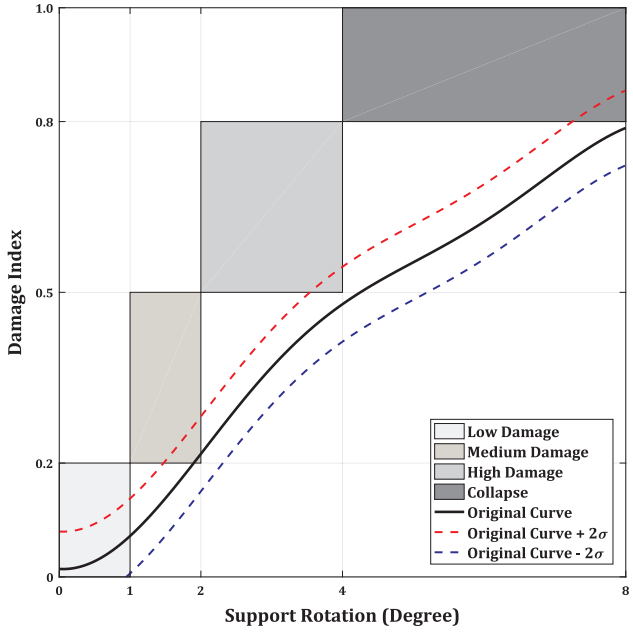

Fig. 15. Comparison of Support rotation and damage index criteria, in the case of negligible axial load.

$$DI(\theta) = \begin{cases} a_0 + \sum_{i=1}^{2} a_i \sin(iw\theta) + \sum_{j=1}^{2} b_j \cos(jw\theta) & 0 \leqslant \theta \leqslant 8^{\circ} \\ Collapse & \theta > 8^{\circ} \end{cases} \quad (14)$$

where θ in degrees is defined based on Eq. (12) and the constant coefficients a_0, a_1, a_2, b_1, b_2 , w are set equal to 0.4411, –0.1081, 0.04541, –0.3407, –0.08643 and 26.41, respectively. By having such a relationship, the post-blast behavior of an H-section steel column (i.e. damage index criterion) can be calculated easily by knowing the support rotation of the member under blast load which can be defined

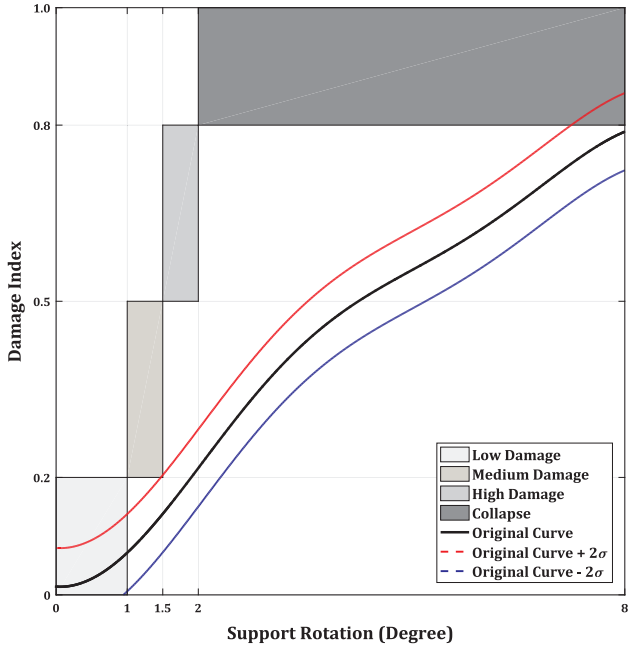

Fig. 16. Comparison of Support rotation and damage index criteria, in the case of significant axial load.

effortlessly using conventional equivalent SDOF system or FE method without need of capturing the post-blast behavior. In addition, another advantage of using the proposed analytical relationship, is that a comparison can be made to find the differences between the acceptance levels given by the support rotation or the damage index criteria.

Figs. 15 and 16 represents in fact the outcomes of Eq. (14), with 95% level of confidence (i.e., mean ± 2σ) and the shaded areas show the levels of damage – low, medium, high and collapse – that have been occurred for both damage index and support rotation criteria, at the same time. Fig. 15 is related to the case in which the initial axial load is negligible (i.e., less than 20% of axial capacity) and maximum allowable support rotation values for low, medium and high damage are 1, 2 and 4 degrees, respectively. Fig. 16, at the same time, refers to the case with an initial axial load that is more than 20% the axial capacity. The corresponding damage levels are 1, 1.5 and 2 degrees respectively, for the mentioned levels. Based on Fig. 15, in the case of negligible compression, it is possible to notice that all the proposed curves are below the shaded areas. This indicates that the support rotation criterion is tougher and overestimates the expected damage levels, which leads stronger design of a given member. According to Fig. 15, it can be also seen that the medium damage scenario, based on support rotation criterion (i.e., 1 to 2 degrees), is equivalent to damage index in the range of 0 to 0.2 degrees, which indicates low damage. Similarly, for high damage based on support rotation criterion (in the range of 2 to 4 degree), damage index is in between 0.2 and 0.5, corresponding to medium damage. Moreover, for support rotations greater than 4 degrees (i.e., collapse), damage index estimates are between 0.5 and 0.8, which indicates high damage. Finally, for support rotation less than 1 degree and more than 8 degree, both support rotation and damage index criteria predict identically low damage or collapse, respectively.

According to Fig. 16, in the case of columns under significant compression, it can be seen that the medium damage scenario based on support rotation criterion (i.e., 1 to 1.5 degrees) is mostly equivalent to damage index in the range of 0 to 0.2, which indicates low damage. Similarly, for high damage given by support rotation (1.5 to 2 degrees), damage index shows approximately a low level of damage. For the case where the support rotation criterion predicts a potential collapse, the damage index criterion varies between medium and high levels. In other words, in the case of columns with an initial axial load more than

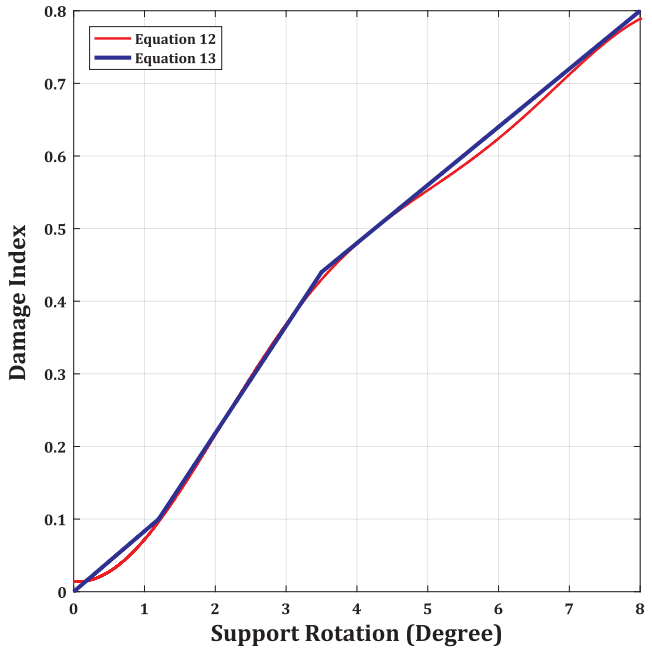

Fig. 17. Comparison of proposed equations for DI(θ) based on Eqs. (14) and (15).

20% of the axial capacity, the support rotation criterion is much conservative than the damage index criterion, which leads unavoidably to stronger design of a given structure.

In addition to the Eq. (14), the following trilinear relationship is also proposed (see Fig. 17) to evaluate damage index based on support rotation which is more practical and simpler compared to the Eq. (14) and it is as follows:

$$DI(\theta) = \begin{cases} 0.0833\theta & 0 \leqslant \theta < 1.2^{\circ} \\ 0.1478\theta - 0.0774 & 1.2^{\circ} \leqslant \theta < 3.5^{\circ} \\ 0.08\theta + 0.16 & 3.5^{\circ} \leqslant \theta < 8.0^{\circ} \\ Collapse & \theta > 8.0^{\circ} \end{cases} \quad (15)$$

8. Calculation examples

In conclusion, to further assess the applicability and potential of the analytical relationships presented in the Section 5.4, some calculation examples are presented to investigate the capability of GEP models in two parts as interpolating and extrapolating. The objective of the example in the first part as interpolating, is to find the initial and residual axial capacities of i) IPB 260 with L = 3200 as Section 1 , and ii) an H-shape steel column with given geometrical properties (b = 250, h = 350, t = 17 , s = 11 and L = 3000 mm) as Section 2. Section 1 is selected from Table 1 while Section 2 is different from the intended sections presented in Table 1 and only have H-shape section with b/h = 0.71. The selected columns are subjected to 700 kN of initial axial load and two different blast scenarios (BS#1 with W = 600 kg TNT at R = 14 m, and BS#2 with W = 350 m, R = 10 m), under the assumption of two idealized boundary conditions, i.e. (a) pinned and (b) fixed end boundary conditions. The material yield stress, density, MoE and Poisson's ratio are set equal to 360 MPa, 7850 kg/m^3, 210 GPa and 0.3, respectively. To determine the initial and residual axial capacities of the selected configurations, the FE method and the practical relationships presented in Tables 6 and 7 and Eqs. (9) and (10) are used separately. The results of such a calculation process are collected in Table 11, for both pinned and fixed ends. As can be seen, the proposed relationships provide good level of accuracy for the estimation of the residual axial capacity of the given members under blast. Such an outcome is further emphasized in the form of percentage scatter between FE estimates (from dynamic explicit analyses) and GEP-derived formulations. Consequently, given the high computational cost of FE explicit simulations (almost 20 min for each run), it is clear that the proposed relationships can be used to obtain practical and reliable estimates. Moreover the proposed equations not only can be used for IPB sections, but also can be implemented to determine the response of other H-shape steel sections.

In terms of damage index of the same columns, the initial axial capacities of the members ($P_{initial}$) must be also calculated. Based on the FE method, it is found that for Section 1, this capacity is in the order of 4613 kN and 4635 kN, for pinned and fixed end conditions respectively. Similarly for Section 2 these values are 4923 and 4938 for pin and fix conditions. Accordingly, the use of practical GEP models for the estimation of $P_{initial}$ (i.e. Eqs. (9) and (10)), turns out in initial capacities equal to 4518 kN and 4567 kN for Section 1 in the case of pin and fix restraints, that result in a maximum scatter of Δ = –2.10% and Δ = –1.49% with respect to FE values. Similarly for Section 2 these values are 4753 and 4801 for pin and fix end conditions with maximum error of Δ = –3.57% and Δ = –2.85% respect to FE values. Damage index values and their corresponding predicted damage levels are provided in Table 12. From this table, the GEP models predict same damage levels respect to FE modelling except for Section 1 under BS#1 and 2, which shows that GEP models have a good accuracy in predicting the damage level of steel column under blast loading. As an example, according to Table 12, for Section 2 under BS#1 with pinned ends, the methods FE and GEP2P predict DI values as 0.06 (or 6%) and 0.13 (or 13%), respectively. From computational point of view, there is a relatively small difference of 7% between the predicted values, and from conceptual one, both methods predict same damage level (i.e. low damage) (same result can be obtained for hypothetical DI values as 0.19 (or 19%) and 0.0 for FE and GEP respectively where there is a difference of 19% between the results of FE and GEP methods but both of them are predicted same damage level). As another example, for Section 1 under BS#2 with pinned ends, the methods FE and GEP2P predict DI values as 0.26 (or 26%) and 0.16 (or 10%), respectively. From computational point of view, there is a relatively small difference of 10% between the predicted values, but from conceptual one, the damage levels predicted by FE and GEP are medium and low respectively which is different to each other (same result can be obtained for hypothetical DI values as 0.21 (or 21%) and 0.19 (or 19%) for FE and GEP, respectively with small difference of 2% and different in predicted damage level). This is because of the way of damage classification where any DI value that is fallen between two boundary values represents only one specific case of damage and the designer' judgment should lead to better comparing the DI results obtained by FE and GEP methods and the choice of damage level for design. Furthermore, as can be seen from Tables 11 and 12, support condition has a significant effect on the response of blast loaded steel columns. By changing the pinned boundary conditions to fixed ends for a given blast load and column geometry, the residual axial capacity increases which consequently decreases the damage index. Considering the fact that real column supports are neither fully pinned nor fixed, the selection of appropriate boundary conditions is thus a key step for reliable FE estimates. Recently, a research study was conducted by Hadianfard and Shekari [32] to investigate the effect of semi-fixed support conditions on the response of flexural members under impact loads. The equivalent SDOF system was used and the transformation factors including load and mass, stiffness and ultimate resistance were obtained for different fixity values in elastic, elastic–plastic and plastic regions. They showed that although considering the semi-fixed support conditions would change the responses, the results were between the results of two ideal assumptions of fully pinned and fully fixed support conditions. Accordingly, based on the separate results for two limit pinned or fixed conditions, the designer' judgment should lead to the choice of a realistic value of residual axial capacity or damage index that best

Table 11
Residual axial capacities for selected steel columns, under BS#1 and BS#2.

		Residual axial capacity $P_{Residual}$ (kN)												
		Pinned ends							Fixed ends					
	BS#	FEM	GEP1P	Δ (%)	GEP2P	Δ (%)	GEP3P	Δ (%)	FEM	GEP1F	Δ (%)	GEP2F	Δ (%)	GEP3F	Δ (%)
Section 1	1	3541	4234	**16.36**	4071	**13.01**	4201	**15.71**	4523	4241	**6.23**	4274	**5.51**	4445	**1.72**
	2	3425	4076	**15.97**	3816	**10.24**	3910	**12.40**	4227	4042	**4.37**	4076	**3.57**	4080	**3.47**
Section 2	1	4625	4293	**7.73**	4131	**10.68**	4258	**7.93**	4735	4307	**9.03**	4339	**8.36**	4512	**4.70**
	2	4231	4038	**4.50**	4031	**4.72**	4312	**1.87**	4652	4278	**8.03**	4302	**7.52**	4336	**6.79**

Table 12
Damage index values and their corresponding predicted damage levels based on GEP models and FE modelling.

		Damage index							
		Pinned ends				Fixed ends			
	BS#	FEM	GEP1P	GEP2P	GEP3P	FEM	GEP1F	GEP2F	GEP3F
Section 1	1	0.23	0.07	0.10	0.06	0.02	0.03	0.06	0.07
		Medium	Low	Low	Low	Low	Low	Low	Low
	2	0.26	0.13	0.16	0.10	0.09	0.11	0.11	0.11
		Medium	Low	Low	Low	Low	Low	Low	Low
Section 2	1	0.06	0.10	0.13	0.10	0.04	0.06	0.10	0.10
		Low	Low	Low	Low	Low	Low	Low	Low
	2	0.14	0.09	0.15	0.15	0.06	0.10	0.10	0.11
		Low	Low	Low	Low	Low	Low	Low	Low

Table 13
Calculating damage index using support rotation values.

		Support Rotation (θ) and Damage Index (DI)											
		Pinned Ends						Fixed ends					
		FEM			SDOF			FEM			SDOF		
	BS#	θ (FEM)	DI (Mean)	DI (95%)	θ (SDOF)	DI (Mean)	DI (95%)	θ (FEM)	DI (Mean)	DI (95%)	θ (SDOF)	DI (Mean)	DI (95%)
Section 1	1	2.10	**0.23**	0.29	1.65	0.14	**0.20**	0.73	**0.06**	0.13	0.38	0.03	**0.10**
	2	3.12	**0.38**	0.45	1.94	0.21	**0.27**	1.33	**0.12**	0.19	0.54	0.04	**0.11**
Section 2	1	0.83	**0.07**	0.14	0.58	0.05	**0.12**	0.27	**0.02**	0.09	0.17	0.01	**0.08**
	2	1.37	**0.13**	0.19	0.79	0.06	**0.13**	0.50	**0.04**	0.11	0.25	0.02	**0.10**

Table 14
Selected configurations and their input values for testing extrapolation capabilities of the proposed GEP models.

		Input variables						
Sample	Section	W_{eff}	R	F_y	A	λ_{max_Pinned}	λ_{max_Fixed}	P_d
1	IPB280	2340	22	180	13100	50.7	25.4	472
2	IPB280	2340	22	550	13100	50.7	25.4	1441
3	IPB140	2340	22	180	4300	100.6	50.3	155
4	IPB140	2340	22	550	4300	100.6	50.3	473

describes the real boundaries [32].

As stated in section 6, the conventional equivalent SDOF system approach can be certainly used to determine damage index of a given member, based on support rotation, as a function of the maximum mid-span displacement (Eq. (12)). In this regard, the equivalent SDOF method has been used for the calculation example, with the support of Matlab software, so as to calculate the support rotation of the selected steel columns. For the sake of brevity, the details of the SDOF method is not reported in this paper (can be found in [14,15]), and only its major results are presented in Table 13. It is possible to notice that at least in some cases, the mean value of DI (i.e., Eq. (14)) is close to the actual

Table 15
Calculating initial and residual axial capacities for selected steel columns in Table 14.

	Pinned						Fixed					
	$P_{residua}$			$P_{initial}$			$P_{residual}$			$P_{initial}$		
Sample	FE	GEP1P	Δ (%)	FE	Eq. 9	Δ (%)	FE	GEP1F	Δ (%)	FE	Eq. 10	Δ (%)
1	2641	1878	28.9	2659	2694	1.3	2648	2646	0.1	2651	2504	5.5
2	7534	9846	23.5	7815	7845	0.4	7758	7631	1.6	7963	7530	5.4
3	496	1159	57.2	856	692	19.2	833	737	11.5	853	924	7.7
4	1912	2957	35.3	2620	2081	20.6	2581	1118	56.7	2625	2738	4.1

value of the damage index presented in Table 12. Otherwise, mostly in SDOF method, the upper limit of the Damage Index with 95% of confidence level (i.e., Eq. (14) + 2 × σ) is close to the actual damage index calculated directly by FE modelling (see Table 12) and damage index calculated by Eq. (14) based on the rotation values obtained from FE modelling. The comprehensive calculations (not included in this paper) showed that the support rotation values obtained by SDOF methods are mostly less than those obtained by FE modelling which leads to lower DI and also damage index fluctuates between two standard deviations. Therefore, in order to be sure about the predicted DI, and to have a more pronounced safety margin, the upper DI limit should be used for calculations.

In the second part, the proposed GEP models have been used also to further evaluate their extrapolation capabilities. In this regard, four samples of steel columns made of IPB140 and IPB280 sections are selected. IPB280 is selected from Table 1 while IPB140 is outside the range of intended sections presented in Table 1. The input parameters including blast load parameters and mechanical properties of steel material with their corresponding values which are beyond the considered ranges (see Table 8) are presented in Table 14 for each selected configuration. The density, MoE and Poisson's ratio are set equal to 7850 kg/m^3, 210 GPa and 0.3, respectively for all samples. The results of residual axial capacities as well as initial axial capacities of the selected examples obtained from FE analyses and GEP models are presented in Table 15 for both pinned and fixed support conditions. Based on Table 15, it can be seen that in some cases the proposed GEP models have accurately predicted the residual axial capacities in comparison with the FE results, while in some other ones the scatters are more than 50%. In case of initial axial capacity, the proposed formulas (i.e. Eqs. (9) and (10)) provide more reliable estimations in comparison with those formulas proposed for calculating residual axial capacity. In the other words, although the proposed GEP models can be used to calculate the initial and residual axial capacity beyond the range of available data, considering the fact that the GEP method is generally based on interpolation within the input dataset, the results may be close to reality or have a significant error. In general, the use of proposed formulas beyond the considered ranges can provide a primary estimation of a member's behavior, but the accuracy of the results should be examined through further studies and engineering judgment.

9. Summary and conclusions

In this paper, the damage evaluation of blast loaded of H-section steel columns were investigated. In this regard, a set of 5600 FE modelling of columns in the range IPB180 to IPB550 with different heights, material properties, boundary conditions and exposed loading were randomly generated and numerically investigated via explicit finite element software LS-DYNA. A set of LS-PrePost, MATLAB, LS-DYNA and C# coding was used to link together for FE modelling, analysing the models and extracting and post-processing the results, automatically. By implementing the gene expression programming, some equations were proposed for finding (a) initial axial capacity of H-section steel columns, and (b) residual axial capacity of blast loaded H-section steel columns. Furthermore, an equation has been proposed to relate the damage index based residual axial capacity to the conventional displacement/rotational index. In addition to FE modelling, the conventional SDOF system was written in Matlab software and used to find the support rotation and post-blast behavior of the columns using the proposed relationship between damage index and support rotation criteria. The following conclusions were obtained:

- The proposed equations for residual axial capacity of blast loaded steel columns for both pinned and fixed ends conditions have a very good agreement with the FE results in training, testing and validating parts and all the GEP models have R^2 values more than 0.94 which indicates a high level of accuracy in predicting the residual axial capacity and can be used to obtain practical and reliable estimates. Moreover the proposed equations can be implemented to determine the response of other H-shape steel sections in addition to IPB sections.
- The proposed equations can be used in the field of reliability analysis of blast loaded steel columns, which demands high numbers of iterations, to reduce the time of analysis.
- Two equations were proposed for determining the initial axial capacities of H-section steel columns with R^2 values more than 0.997 for both cases of pinned and fixed conditions which indicate very satisfactory accuracy in predicting the initial capacity with approximately maximum scatter of 3.57% respect to FE modelling.
- The results of sensitivity analyses showed that by increasing the R and AF_y parameters, the residual axial capacity increases, whereas by increasing the W_{eff} and λ_{max} values, the residual axial capacity decreases. Furthermore, P_d had negligible effect on the residual axial capacity values compared to other input parameters and AF_y was the most effective parameter in the proposed GEP models.
- An equation was proposed with R^2 value of 0.957, to relate the damage index based residual axial capacity to the conventional displacement/rotational index which can be obtained effortlessly by conventional equivalent SDOF system or FE modelling without need of capturing the post-blast behavior of the column. Additionally a trilinear relationship was also proposed which is more practical and simpler compared to the other one.
- The results indicated that the support rotation criterion is much conservative than the damage index criterion, which leads unavoidably to stronger design of a given structure.
- The results showed that conventional equivalent SDOF method can be used to find the support rotation of the column and consequently the post-blast behavior of column by proposed relationship with a good level of accuracy and less computational time effort. In this regard, in order to be sure about the predicted DI based on SDOF method, and to have a more pronounced safety margin, the upper DI limit should be used for calculations.

CRediT authorship contribution statement

Mohammad Momeni: Methodology, Software, Investigation, Validation, Formal analysis, Writing - original draft. **Mohammad Ali Hadianfard:** Project administration, Supervision, Conceptualization, Methodology, Validation, Writing - review & editing. **Chiara Bedon:** Supervision, Validation. **Abdolhossein Baghlani:** Supervision, Validation.

Acknowledgments

The authors wish to thank Sina Malekpour from Shiraz University of Technology for his precious and constructive comments.

References

[1] Nassr AA, Razaqpur AG, Tait MJ, Campidelli M, Foo S. Dynamic response of steel columns subjected to blast loading. J Struct Eng 2013;140(7):04014036.
[2] Nassr AA, Razaqpur AG, Tait MJ, Campidelli M, Foo S. Strength and stability of steel beam columns under blast load. Int J Impact Eng 2013;55:34–48.
[3] Magallanes JM, Martinez R, Koenig JW. Experimental results of the AISC full-scale column blast test. Rep. TR-06, vol. 20; 2006.
[4] Nassr AA, Razaqpur AG, Campidelli M. Effect of initial blast response on RC beams failure modes. Nucl Eng Des 320;2017:437-451 [2017/08/15/ 2017].
[5] Rong H-C, Li B. Probabilistic response evaluation for RC flexural members subjected to blast loadings. Struct Saf 2007;29(2):146–63.
[6] Yokoyama T. Limits to deflected shape assumptions of the SDOF methodology for analyzing structural components subject to blast loading. J Perform Constr Facil 2014;29(5):B4014008.
[7] Crawford JE, Magallanes JM. The effects of modeling choices on the response of structural components to blast effects. Int J Protect Struct 2011;2(2):231–66.
[8] Al-Thairy H. A modified single degree of freedom method for the analysis of building steel columns subjected to explosion induced blast load. Int J Impact Eng 2016;94:120–33.

[9] Lee K, Kim T, Kim J. Local response of W-shaped steel columns under blast loading. Struct Eng Mech 2009;31(1):25–38.
[10] Shi Y, Hao H, Li Z-X. Numerical derivation of pressure–impulse diagrams for prediction of RC column damage to blast loads. Int J Impact Eng 2008;35(11):1213–27.
[11] Hadianfard MA, Farahani A. On the effect of steel columns cross sectional properties on the behaviours when subjected to blast loading. Struct Eng Mech 2012;44(4):449–63.
[12] Hadianfard MA, Nemati A, Johari A. Investigation of steel column behavior with different cross section under blast loading. Modares Civil Eng J 2016;16(4):265–78.
[13] Figuli L, Bedon C, Zvaková Z, Jangl Š, Kavický V. Dynamic analysis of a blast loaded steel structure. Procedia Eng 2017;199:2463–9.
[14] DoD U. Structures to resist the effects of accidental explosions. US DoD, Washington, DC, USA. UFC 3-340-022008.
[15] Bounds WL. Design of blast-resistant buildings in petrochemical facilities. ASCE Publications; 2010.
[16] Bao X, Li B. Residual strength of blast damaged reinforced concrete columns. Int J Impact Eng 2010;37(3):295–308.
[17] Li B, Nair A, Kai Q. Residual axial capacity of reinforced concrete columns with simulated blast damage. J Perform Constr Facil 2012;26(3):287–99.
[18] Abedini M, Mutalib A, Raman S, Baharom S, Nouri J. Prediction of residual axial load carrying capacity of reinforced concrete (RC) columns subjected to extreme dynamic loads. Am J Eng Appl Sci 2017;10:431–48.
[19] Abedini M, Mutalib AA. Investigation into damage criterion and failure modes of RC structures when subjected to extreme dynamic loads. Arch Computat Methods Eng; 2019. p. 1–15.
[20] Park JY, Kim MS, Scanlon A, Choi H, Lee YH. Residual strength of reinforced concrete columns subjected to blast loading. Mag Concr Res 2014;66(2):60–71.
[21] Wu K-C, Li B, Tsai K-C. Residual axial compression capacity of localized blast-damaged RC columns. Int J Impact Eng 2011;38(1):29–40.
[22] Wijesundara LM, Clubley SK. Residual axial capacity of reinforced concrete columns subject to internal building detonations. Int J Struct Stab Dyn 2016;16(08):1550050.
[23] Li J, Wu C, Hao H. Residual loading capacity of ultra-high performance concrete columns after blast loads. Int J Protect Struct 2015;6(4):649–69.
[24] Li J, Wu C, Hao H, Liu Z. Post-blast capacity of ultra-high performance concrete columns. Eng Struct 2017;134:289–302.
[25] Li M, Zong Z, Liu L, Lou F. Experimental and numerical study on damage mechanism of CFDST bridge columns subjected to contact explosion. Eng Struct 2018;159:265–76.
[26] Chen W, Zhou Z, Zou H, Guo Z. Predictions of residual carrying-capacities for fire and near-field blast-damaged reactive powder concrete-filled steel tube columns. Int J Protect Struct 2018;9(4):525–53.
[27] Zhang F, Wu C, Li Z-X, Zhao X-L. Residual axial capacity of CFDST columns infilled with UHPFRC after close-range blast loading. Thin-Walled Struct 2015;96:314–27.
[28] Zhang F, Wu C, Zhao X-L, Li Z-X. Numerical derivation of pressure-impulse diagrams for square UHPCFDST columns. Thin-Walled Struct 2017;115:188–95.
[29] Momeni M, Hadianfard MA, Baghlani A. Implementation of weighted uniform simulationmethod in failure probability analysisof steel columns under blast load. In: presented at the 11th International Congress on Civil Engineering, University of Tehran, Iran; 2018.
[30] Hadianfard MA, Malekpour S. Evaluation of explosion safe distance of steel column via structural reliability analysis. Adv Def Sci Technol 2018;8(4):349–59.
[31] Hadianfard MA, Malekpour S, Momeni M. Reliability analysis of H-section steel columns under blast loading. Struct Saf 2018;75:45–56.
[32] Hadianfard MA, Shekari M. An equivalent single-degree-of-freedom system to estimate nonlinear response of semi-fixed flexural members under impact load. Iran J Sci Technol Trans Civil Eng; 2018. p. 1–13.
[33] Momeni M, Hadianfard MA, Bedon C, Baghlani A. Numerical damage evaluation assessment of blast loaded steel columns with similar section properties. Structures 2019;20:189–203.
[34] Cui J, Shi Y, Li Z-X, Chen L. Failure analysis and damage assessment of rc columns under close-in explosions. J Perform Constr Facil 2015;29(5):B4015003.
[35] Wu K-C, Li B, Tsai K-C. The effects of explosive mass ratio on residual compressive capacity of contact blast damaged composite columns. J Constr Steel Res 2011;67(4):602–12.
[36] Johari A, Habibagahi G, Ghahramani A. Prediction of soil–water characteristic curve using genetic programming. J Geotech Geoenviron Eng 2006;132(5):661–5.
[37] Johari A, Nejad AH. Prediction of soil-water characteristic curve using gene expression programming. Iran J Sci Technol Trans Civil Eng 2015;39(C1):143.
[38] Alkroosh I, Nikraz H. Correlation of pile axial capacity and CPT data using gene expression programming. Geotech Geol Eng 2011;29(5):725–48.
[39] Shahin MA. Artificial intelligence in geotechnical engineering: applications, modeling aspects, and future directions. Metaheuristics in Water, Geotechnical and Transport Engineering, X. Yang, A. H. Gandomi, S. Talatahari, and A. H. Alavi, Elsevier Inc., London; 2013. p. 169–204.
[40] Shahin MA, Maier HR, Jaksa MB. Data division for developing neural networks applied to geotechnical engineering. J Comput Civil Eng 2004;18(2):105–14.
[41] Alkroosh I, Nikraz H. Predicting pile dynamic capacity via application of an evolutionary algorithm. Soils Found 2014;54(2):233–42.
[42] Hadianfard MA, Jafari S. Prediction of lightweight aggregate concrete compressive strength using ultrasonic pulse velocity test through gene expression programming. Scientia Iranica. Transaction A: Civil Engineering 2016;23(6):2506–13.
[43] Jafari S, Mahini SS. Lightweight concrete design using gene expression programing. Constr Build Mater 2017;139:93–100.
[44] Güneyisi EM, Nour AI. Axial compression capacity of circular CFST columns transversely strengthened by FRP. Eng Struct 2019;191:417–31.
[45] Stewart L, Morrill K. Residual capacity prediction of blast-loaded steel columns using physics-based fast running models. Int J Saf Secur Eng 2015;5(4):289–303.
[46] Remennikov AM, Rose TA. Predicting the effectiveness of blast wall barriers using neural networks. Int J Impact Eng 2007;34(12):1907–23.
[47] Bewick B, Flood I, Chen Z. A neural-network model-based engineering tool for blast wall protection of structures. Int J Protect Struct 2011;2(2):159–76.
[48] Hosseini SA, Tavana A, Abdolahi SM, Darvishmaslak S. Prediction of blast-induced ground vibrations in quarry sites: a comparison of GP, RSM and MARS. Soil Dyn Earthq Eng 2019;119:118–29.
[49] Shin J, Scott DW, Stewart LK, Jeon J-S. Multi-hazard assessment and mitigation for seismically-deficient RC building frames using artificial neural network models. Eng Struct 2020;207:110204.
[50] Shishegaran A, Khalili MR, Karami B, Rabczuk T, Shishegaran A. Computational predictions for estimating the maximum deflection of reinforced concrete panels subjected to the blast load. Int J Impact Eng 2020;139:103527.
[51] Cowper GR, Symonds PS. Strain-hardening and strain-rate effects in the impact loading of cantilever beams. Brown Univ Providence Ri1957.
[52] Jones N. Structural impact. Cambridge University Press. Cambridge, UK; 1989.
[53] Shi Y, Stewart MG. Spatial reliability analysis of explosive blast load damage to reinforced concrete columns. Struct Saf 2015;53:13–25.
[54] Li J, Hao H, Wu C. Numerical study of precast segmental column under blast loads. Eng Struct 2017;134:125–37.
[55] Mutalib AA, Hao H. Development of PI diagrams for FRP strengthened RC columns. Int J Impact Eng 2011;38(5):290–304.
[56] FEMA F. 426: Reference Manual to Mitigate Potential Terrorist Attacks Against Buildings-Buildings and Infrastructure Protection Series. Federal Emergency Management Agency; 2003.
[57] Kennett M, Letvin E, Chipley M, Ryan T. FEMA 452-Risk Assessment. Federal Emergency Management Agency; 2005.
[58] Beshara F. Modelling of blast loading on aboveground structures—I. General phenomenology and external blast. Comput Struct 1994;51(5):585–96.
[59] S S. S. Design. Analysis Handbook. US Army Corps of Engineers, Huntsville Division, HNDM-1110-1-2; 1977.
[60] Karlos V, Solomos G. Calculation of blast loads for application to structural components. Luxembourg: Publications Office of the European Union; 2013.
[61] Kelliher D, Sutton-Swaby K. Stochastic representation of blast load damage in a reinforced concrete building. Struct Saf 2012;34(1):407–17.
[62] Krauthammer T. Blast effects and related threats. Penn State University; 1999.
[63] Karlos V, Solomos G, Larcher M. Analysis of the blast wave decay coefficient using the Kingery-Bulmash data. Int J Protect Struct 2016;7(3):409–29.
[64] Koza JR. Genetic programming: on the programming of computers by means of natural selection. MIT press; 1992.
[65] Ferreira C. Gene expression programming in problem solving. In: Soft computing and industry. Springer; 2002. p. 635–653.
[66] Bowden GJ, Nixon JB, Dandy GC, Maier HR, Holmes M. Forecasting chlorine residuals in a water distribution system using a general regression neural network. Math Comput Modell 2006;44(5–6):469–84.
[67] GeneXproTools. Version 5.0; http://www.gepsoft.com.
[68] Nazari A, Rajeev P, Sanjayan JG. Modelling of upheaval buckling of offshore pipeline buried in clay soil using genetic programming. Eng Struct 2015;101:306–17.
[69] Ferreira C. Gene expression programming: mathematical modeling by an artificial intelligence. Springer; 2006.
[70] Masters T. Practical neural network recipes in C++. Morgan Kaufmann; 1993.
[71] Alkroosh IS, Bahadori M, Nikraz H, Bahadori A. Regressive approach for predicting bearing capacity of bored piles from cone penetration test data. J Rock Mech Geotech Eng 2015;7(5):584–92.
[72] Gandomi AH, Alavi AH, Gandomi M, Kazemi S. Formulation of shear strength of slender RC beams using gene expression programming, part II: With shear reinforcement. Measurement 2017;95:367–76.
[73] Gandomi AH, Tabatabaei SM, Moradian MH, Radfar A, Alavi AH. A new prediction model for the load capacity of castellated steel beams. J Constr Steel Res 2011;67(7):1096–105.
[74] David M. Statistics for Managers, Using Microsoft Excel. Pearson Education India; 2017.
[75] Johari A, Momeni M. Stochastic analysis of ground response using non-recursive algorithm. Soil Dyn Earthquake Eng 2015;69:57–82.
[76] Johari A, Momeni M, Javadi A. An analytical solution for reliability assessment of pseudo-static stability of rock slopes using jointly distributed random variables method; 2015.
[77] A. I. o. S. Construction. Specification for structural steel buildings; 2016.